UNIVERSITÀ DEGLI STUDI DI PADOVA

CORSO DI LAUREA MAGISTRALE IN MEDICINA E CHIRURGIA

DIPARTIMENTO DI NEUROSCIENZE

Direttore: Prof. Raffaele De Caro

CLINICA NEUROLOGICA

Direttore: Prof. Maurizio Corbetta

TESI DI LAUREA

THE ROLE OF OPTICAL COHERENCE TOMOGRAPHY (OCT) AND SKIN BIOPSY IN THE DIAGNOSIS AND FOLLOW-UP OF PARKINSON'S DISEASE AND MULTIPLE SYSTEM ATROPHY: LOOKING FOR POSSIBLE EARLY BIOMARKERS

RELATORE: Prof. Angelo Antonini

CORRELATORI: Dott.ssa Marta Campagnolo

Dott. Aron Emmi

LAUREANDA: Beatrice Maccari

ANNO ACCADEMICO 2022/2023

CONTENTS

RIASSUNTO……....1

ABSTRACT……...3

1. Introduction..... 5

1.1 α-synucleinopathies..... 5

1.2 Parkinson's Disease (PD)..... 6

1.2.1 Epidemiology..... 6

1.2.2 Neuropathology..... 7

1.2.3 Clinical presentation..... 9

1.2.4 Diagnosis..... 11

1.2.5 Differential Diagnosis..... 14

1.2.6 Prognosis..... 18

1.2.7 Treatment..... 18

1.3 Multiple System Atrophy (MSA)..... 21

1.3.1 Epidemiology..... 21

1.3.2 Neuropathology..... 22

1.3.3 Clinical presentation..... 23

1.3.4 Diagnosis..... 24

1.3.5 Differential diagnosis..... 26

1.3.6 Prognosis..... 27

1.3.7 Treatment..... 27

1.4 New biomarkers in α-synucleinopathies..... 28

1.4.1 Fluid biomarkers..... 29

1.4.2 Skin biopsy..... 32

1.4.3 Optical Coherence Tomography..... 34

2. Aim of the study..... 41

3. Materials and methods.....43

3.1 Population.....43

3.2 Clinical evaluation.....43

3.3 Optical coherence tomography.....46

3.5 Skin biopsy.....50

3.5.1 RT-QuIC.....50

3.5.2 Histopathological evaluation.....51

3.6 Statistical analysis.....53

4. Results.....55

4.1 Clinical characteristics of the study population.....55

4.2 Clinical evaluation.....56

4.3 Optical coherence tomography.....58

4.4 Skin biopsy.....61

5. Discussion.....65

6. Conclusions.....69

7. Bibliography.....71

RIASSUNTO

Presupposti: Come dimostrato dal lungo ritardo diagnostico (in media 10 anni), le prime fasi della malattia di Parkinson (PD) sono difficili da identificare. Anche la diagnosi differenziale di tale malattia, soprattutto con altre α-sinucleinopatie, può risultare complessa, soprattutto in fase precoce. Nell'atrofia multisistemica (MSA), la presentazione clinica con sintomi prevalentemente non-motori all'esordio della malattia può essere indistinguibile da quella di altre α-sinucleinopatie. Inoltre, con l'avvento della medicina personalizzata, emerge la necessità di trovare dei predittori prognostici per poter valutare la progressione della malattia in ogni paziente.

Scopo dello studio: Definire il possibile ruolo della tomografia a coerenza ottica (OCT) e della biopsia di cute come biomarkers nella diagnosi precoce e nel follow-up di PD e MSA. Validare OCT e biopsia di cute come strumenti nella diagnosi differenziale delle α-sinucleinopatie.

Materiali e metodi: Pazienti con PD, MSA e controlli sani (HC) sono stati sottoposti a OCT. I pazienti con PD e MSA, inoltre, sono stati valutati clinicamente usando le scale, rispettivamente, MDS-UPDRS e UMSARS per determinare il grado di malattia e con la scala COMPASS 31 per la stima della disautonomia e sono stati sopposti a biopsia di cute analizzata sia con immunoistochimica (IHC) che con *real-time quaking-induced conversion* (RT-QuIC).

Risultati: Abbiamo analizzato le scansioni OCT di 24 pazienti PD, 12 pazienti MSA e 10 HC. Il numero di foci iperriflettenti retinici (HRF), un potenziale *marker* di attivazione della microglia, è risultato significativamente maggiore nei sottogruppi patologici (PD>MSA) rispetto agli HC. Il rilevamento tramite IHC di α-syn nelle biopsie di cute è stato in grado di identificare i soggetti malati con buona sensibilità (71% in PD e 67% in MSA). I punteggi RT-QuIC dei pazienti con PD hanno mostrato una correlazione lineare sia con la gravità della malattia (UPDRS II, UPDRS III, punteggio totale UPDRS) che con i sintomi autonomici (domini relativi a ipotensione ortostatica e sintomi genitourinari della scala validata COMPASS 31).

Conclusioni: Gli HRF sono significativamente aumentati nei sottogruppi patologici (PD>MSA). La biopsia di cute analizzata tramite IHC mostra buona

sensibilità. Gli *score* RT-QuIC correlano con grado di malattia e sintomi autonomici. Si può, dunque, concludere che sia l'OCT che la biopsia cutanea possono essere considerati potenziali biomarkers nella diagnosi precoce e nel follow-up delle α-sinucleinopatie.

ABSTRACT

Background: The identification of Parkinson's Disease (PD) in the early stages might be challenging, as demonstrated by the long diagnostic delay (on average 10 years) in the majority of patients. The differential diagnosis, especially with other α-synucleinopathies, may also be difficult. In multiple system atrophy (MSA), non-motor features, predominant at disease onset, may be indistinguishable from other α-synucleinopathies. Moreover, with the rise of personalized medicine, new prognostic and predictive markers are needed in order to assess disease progression.

Aim of the study: To define the possible role of optical coherence tomography (OCT) and skin biopsy as biomarkers in the early diagnosis and follow-up of PD and MSA. To validate OCT and skin biopsy as possible tools in the differential diagnosis of α-synucleinopathies.

Methods: OCT was performed in patients with PD, MSA and in healthy controls (HC). PD and MSA patients were clinically evaluated with, respectively, MDS-UPDRS and UMSARS scores in order to assess disease severity and with COMPASS 31 to estimate autonomic dysfunction. Pathological subgroups (PD and MSA) also underwent skin biopsy, analyzed both via immunohistochemistry (IHC) and real-time quaking-induced conversion (RT-QuIC).

Results: We analyzed OCT scans from 24 PD patients, 12 MSA patients and 10 HCs. The number of hyperreflective foci (HRF), a potential marker for microglial activation, was significantly greater in the pathological subgroups (PD>MSA) than in the HCs. IHC detection of α-syn in skin punch biopsies was able to identify diseased subjects with good sensitivity (71% in PD and 67% in MSA). RT-QuIC scores of PD patients showed a linear correlation with both disease severity (UPDRS II, UPDRS III, UPDRS total score) and autonomic symptoms (orthostatic hypotension and genitourinary domains of the validated COMPASS 31 scale).

Conclusion: HRF are significantly increased in pathological subgroups (PD>MSA). IHC detection of α-syn in skin punch biopsies showed good sensitivity. RT-QuIC scores correlate with both disease severity and autonomic symptoms. It can be concluded that both OCT and skin biopsy can be considered potential biomarkers in the early diagnosis and follow-up of α-synucleinopathies.

1. Introduction

1.1 α-synucleinopathies

α-synucleinopathies are a group of neurodegenerative disorders, including Parkinson's Disease (PD), Dementia with Lewy bodies (DLB) and Multiple system atrophy (MSA) characterized by the deposition of insoluble aggregates of pathological α-synuclein (α-syn) in neuronal or glial cells in different regions of the central (CNS) and peripheral nervous system (PNS) (1).

α-syn belongs to a family of proteins including also β-synuclein (β-syn) and γ-synuclein (γ-syn), presenting with a highly conserved α-helical lipid-binding motif, that is very similar to the class-A2 lipid-binding domains of the exchangeable apolipoproteins. While β-syn is mostly located in the presynaptic terminals, γ-syn is expressed in the retina and PNS (2). α-syn is a small (14 KDa) acidic protein expressed in the neurons of both the CNS and PNS as well as in the hematopoietic tissue (i.e., erythrocytes, megakaryocytes, platelets, lymphocytes, and monocytes) and -in lower concentrations- in the heart, placenta, lungs, kidneys, skeletal muscles, pancreas, and liver (3,4). α-syn plays a crucial role in the presynaptic regulation of the SNARE complex, involved in trafficking and recycling, (5) and in the membrane biogenesis mechanisms (6). By inhibiting the synthesis of dopamine (DA) and promoting both the storage of the neurotransmitter in the presynaptic vesicles and the extracellular reuptake of the compound, α-syn functions as a major regulator of the dopamine metabolism in neurons (7).

In PD and DLB, α-syn adopts a pathological β-sheet conformation that recruits additional monomers to form oligomers and amyloid fibrils. In these disorders, α-syn inclusions localize in neurons (both in axons forming Lewy neurites, or in the soma, creating Lewy Bodies), as opposed as in MSA, where α-syn aggregates form cytoplasmic argyrophilic inclusions called Papp-Lantos bodies (3). It is still unclear why this protein undergoes misfolding but several mechanisms appear to be involved including phosphorylation of S129 and other residues localized at the C-terminal region of the protein and mutations in the α-syn gene (SNCA) (8,9). Moreover, alterations in the main degradation systems [the ubiquitin-proteasome

system (UPS) and the autophagy-lysosome pathway] observed in in-vivo studies (10) seem to contribute significantly to α-syn misfolding and deposition (11).

Several studies have suggested a prion-like mechanism of propagation of the misfolded α-syn in PD, mirroring the mechanisms proposed in other neurodegenerative disorders such as Alzheimer disease (AD) and frontotemporal dementia (FTD), with the common ground constituted by the deposition of fibrillar aggregates of proteins [tau, amyloid-β (Aβ) and α-syn]. According to this theory, fibrillar proteins (likely formed by splice isoforms or proteins with post-translational changes) seeds from adjacent or synaptically connected cells could cause the aggregation of properly structured protein. Moreover, these findings might explain both the phenotypic diversity seen in sporadic neurodegenerative diseases, in which a single protein underlies a variety of conditions, and the spread of the pathologic process, in which aggregates are capable of migrating between cells to propagate misfolding (12).

1.2 Parkinson's Disease (PD)

PD is a neurodegenerative disorder characterized by the progressive dysfunction of dopaminergic neurons in the basal ganglia, particularly the substantia nigra pars compacta. Parkinsonism, a clinical syndrome including bradykinesia as well as resting tremor and/or rigidity, is a key clinical feature of PD.

1.2.1 Epidemiology

It is estimated that PD has a worldwide incidence ranging from 5 to >35 new cases per 100.000 individuals with around 6.1 million patients with a confirmed diagnosis in 2016 (13). The prevalence, which is estimated to be 0.3% worldwide, rises to >3% in subjects >80 years old (14). Men are more likely to have PD (1.4:1.0 male-to-female ratio), with an onset usually after 50 years of age.

Although the great majority of patients are defined as idiopathic, genetic and environmental factors such as exposure to pesticides, herbicides, and heavy metals are known to play a role (15,16). Only about 10% of patients with PD have a positive family history with mutations in the SNCA (PARK1 = 4), and LRRK2 (PARK8) genes being accountable for the majority of autosomal-dominant PD forms, and Parkin (PARK2), PINK1 (PARK6), DJ-1 (PARK7), and ATP13A2 (PARK9) mutations being responsible for PD forms with an autosomal recessive mode of inheritance. These six genes are unquestionably linked to heritable, monogenic PD. However, they only represent about 30% of familial and 3% to 5% of sporadic occurrences (17). Therefore, ongoing scientific research is attempting to discover other mutations linked to genetic PD.

1.2.2 Neuropathology

From the neuropathological point of view, PD is characterized by a progressive degeneration of the dopaminergic neurons in the substantia nigra pars compacta in the basal ganglia.

The Lewy bodies, neuronal inclusions primarily formed by α-syn aggregates, are the pathologic hallmark of PD.

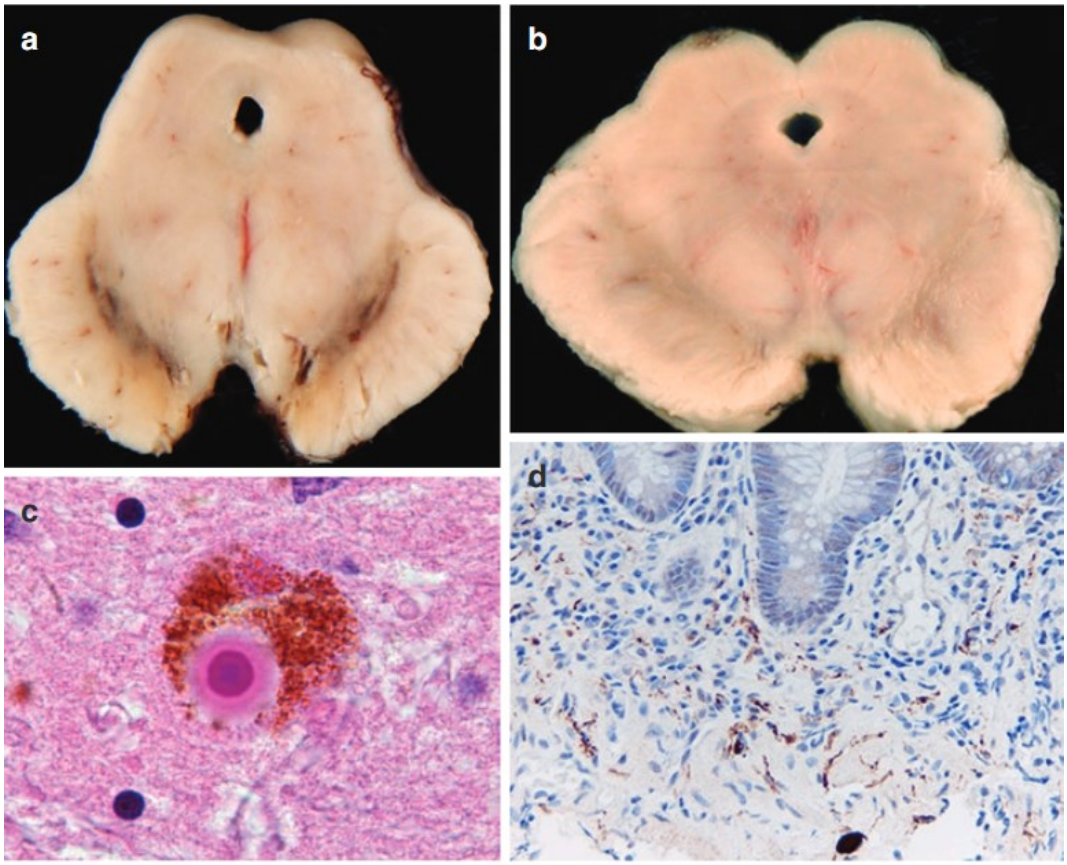

Fig.1 - (a) Normal midbrain. (b) PD pallor of substantia nigra due to loss of pigmented neurons. (c) Lewy body within the pigmented neuron of substantia nigra. H&E stain. (d) Deposition of α-synuclein within small autonomic nerves of bowel before the onset of neurological symptoms. Adapted from: Hilton et al., Neurodegenerative Disorders (18)

According to the α-syn prion-like hypothesis, once the pathological aggregates have developed in a neuron, they can be transported intra-axonally to other parts of the CNS, released into the extracellular space, taken up by nearby neurons, and then seed the aggregation of endogenous α-syn once inside their new cellular host (14). According to the Braak hypothesis (19), the pathological α-syn aggregates initially originate in the enteric or PNS and invade the CNS via retrograde vagal transport. The medulla and the olfactory bulb are the initial localization of the neurodegenerative process (stages 1 and 2). Rapid eye movement sleep behaviour disorder (RBD), in which individuals lose their normal REM sleep paralysis and physically act out their dreams while they are asleep, and impaired smell are symptoms linked to these early stages. Later, the substantia nigra pars compacta, along with other midbrain and basal forebrain regions, are involved with predominant motor symptoms (stages 3 and 4). However, new evidence (20)

suggests that not all PD patients can be reconciled with this hypothesis. It is hypothesized that PD can be divided into a PNS-first and a CNS-first subtype. The former is associated with RBD during the prodromal phase and is characterized by autonomic damage before involvement of the dopaminergic system. In contrast, the CNS-first phenotype is usually RBD-negative during the prodromal phase and characterized by nigrostriatal dopaminergic dysfunction prior to involvement of the autonomic PNS.

Neuronal degeneration with Lewy bodies formation can also affect cholinergic neurons of the nucleus basalis of Meynert (NBM), norepinephrine neurons of the locus coeruleus (LC), serotonin neurons in the raphe nuclei of the brainstem, and neurons of the olfactory system, cerebral hemispheres, spinal cord, and peripheral autonomic nervous system. The non-dopaminergic pathology is likely responsible for the development of the non-motor clinical features such as anosmia, mood disorders (e.g., depression), autonomic disturbances, dementia, etc. (21)

1.2.3 Clinical presentation

When dopamine levels in the striatum fall below 60–70%, PD motor manifestations start to present focally, usually involving one limb. The beginning of motor symptoms is correlated with dopamine loss in the posterior putamen, which corresponds to the striatum's motor area.

From the clinical point of view, PD is characterized by three key features: bradykinesia, rest tremor and rigidity (22).

- Bradykinesia: slowness of movements with a progressive loss of speed or amplitude during attempted rapid alternating motions of body parts. It can be tested by having patients perform repeated movements (such as tapping their thumb and index fingers, or tapping their foot on the floor) as fast and widely as they can and by examining the patient's spontaneous movements while sitting, getting up from a chair, or walking. Hypomimia (reduced facial expression and eye blinking); hypophonia (softer voice); micrographia (progressively smaller handwriting); and difficulty swallowing are other clinical manifestations of bradykinesia.

- Rest tremor: an involuntary rhythmic oscillatory movement that occurs when the affected body part is relaxed and resting on a surface. It disappears with movement. Its frequency typically falls in the low to mid-range (3 – 6 Hz). The so-called "pill-rolling" form of tremor, which is visually represented by the simultaneous rubbing movements of the thumb and index fingers against each other, is the most characteristic tremor in PD. Tongue, jaw, and lower limbs can also exhibit tremor. In clinical practice, it is easier to detect tremor when patients are concentrating on a specific mental task (such as counting backwards from 100 with their eyes closed), which promotes limb muscles relaxation.
- Rigidity: an increase in muscular tone (involving both flexor and extensor muscles) that can be felt when examining the passive movement of the segment (limbs or neck). The increase in resistance depends on velocity and is more apparent when the examined joint is stretched slowly; rapid displacement is linked to minimal or no rigidity. When resting tremor coexists, passive limb mobilization can produce the classic "cog wheel rigidity". By voluntary movement of other body parts, the examined segment's rigidity is often increased (Froment's maneuver).

PD patients frequently assume a stooped posture due to the loss of postural reflexes. Extreme anterior truncal flexion (camptocormia) may occur. Parkinsonian gait is slow, occurs on a narrow base, and is characterized by short shuffling steps. Reduced arm swing, slow turning around, and gait freezing can all occur. Festination, which is a condition where a rapid succession of steps is noticed and the patient occasionally is only able to halt when encountering an impediment, can also be seen (23,24).

Non-motor symptoms are predominant in the early stages of the disease, with some of them appearing even before motor involvement. The non-motor symptoms include dysautonomia [manifesting as orthostatic hypotension (OH), sialorrhea, gastrointestinal, urinary, and sexual dysfunctions)], neuropsychiatric features (mood disorders, including depression, anxiety and hallucinations), pain, fatigue, cognitive impairment/dementia and sleep disorders (particularly RBD) (21,24). Olfactory impairment has been described in the great majority of PD patients, with hyposmia or anosmia observed in more than 90% of patients, often preceding the beginning of the dopamine deficiency-related motor symptoms. Although

hyposmia is not typically reported by patients, the presence or advancement of hyposmia could be a biomarker for early premotor PD, especially if it is accompanied by other early clinical features, imaging and/or biomarkers (25). As demonstrated by the long diagnostic delay (on average 10 years) between a patient's first noticeable symptom and the time of diagnosis, the early stages of PD can be challenging to identify. The beginning of clinically manifest motor symptoms may be preceded by a protracted prodromal phase. Idiopathic RBD (iRBD), which is rare but quite specific, is the prodromal symptom with the highest probability of phenoconversion to overt PD (26). A meta-analysis by Galbiati et al. (27) confirmed that there is a risk higher than 90% at 14 years that iRBD will convert to a neurodegenerative disease, mostly a synucleinopathy.

1.2.4 Diagnosis

The diagnosis of PD is based on the presence of the key clinical features. The International Parkinson and Movement Disorder Society (MDS) has proposed a set of criteria that represent a revised version of the Queens Square Brain Bank (QSBB) Criteria (the most widely used in the past decades) in order to increase the diagnostic accuracy in PD (28). These requirements are a clinical neurological examination demonstrating a parkinsonian syndrome as well as the use of other supportive features. Moreover, the MDS criteria include clinical characteristics that are considered atypical in PD and should prompt suspicion of potential alternative diagnosis ('red flags') (29).

The key clinical diagnostic features for PD are bradykinesia + rest tremor (4-6Hz) and/or limb rigidity. For “clinically established” PD (i.e., certainty based on clinical presentation but not on pathologic confirmation), patients also need to meet at least 2 out of 4 supportive criteria:

1. rest tremor of a limb;
2. a dramatic improvement with dopaminergic therapy (e.g., carbidopa-L-dopa);
3. L-dopa-induced dyskinesias (involuntary dance-like choreoathetoid movements);

4. the presence of either olfactory loss or cardiac sympathetic denervation on iodine-123-meta-iodobenzylguanidine myocardial (MIBG) scintigraphy (an imaging test that assesses cardiac norepinephrine uptake, which depends on intact postganglionic sympathetic neuron function [decreased in PD]) (10).

Suppl. material - MDS Criteria for a Clinical Diagnosis of PD (Postuma et al. 2015)
Presence of a parkinsonian syndrome by expert clinical exam • *Bradykinesia* plus at least one out of: • *4-6-Hz rest tremor, limb rigidity*
Supportive clinical criteria • Excellent response to levodopa • Presence of levodopa-induced dyskinesia • Rest tremor of a limb • Presence of either olfactory loss or sympathetic cardiac denervation (MIBG scintigraphy)
Exclusion criteria • Unequivocal cerebellar signs • Downward vertical gaze palsy • Diagnosis of FTD (*behavioral variant or PPA*) within 5 years • Parkinsonism restricted to legs for > 3 yrs. • Exposure to anti-DA drugs consistent with (dose, timing) drug-induced parkinsonism • Absence of L-Dopa response • Cortical sensory loss, limb apraxia, progressive aphasia • Normal functional imaging of presynaptic DA system
'Red Flags' for alternative Dx • Rapid progression of gait impairment (wheelchair within five years) • No progression over 5 yrs • Severe dysphonia, dysarthria or dysphagia within 5 years. • Inspiratory stridor • Severe autonomic failure within 5 years (symptomatic OH, urinary incontinence or retention) • Recurrent falls within 3 years • Disproportionate antecollis or limb contractures within 10 years • Absence of typical PD non-motor symptoms over 5 years • Persistent motor symmetry
Clinically Established PD • Anchored on bradykinesia plus at least one out of rest tremor and rigidity • At least 2 supportive criteria • No exclusion criteria • No "red flags"
Clinically Probable PD • Anchored on bradykinesia plus at least one out of rest tremor and rigidity • No exclusion criteria • Presence of maximally 2 red flags' which must be counterbalanced by equal number of supportive criteria
*Abbreviations: MIBG 123 I-MIBG Myocardial Scintigraphy; FTD frontotemporal dementia; PPA primary progressive aphasia; DA Dopamine; PD Parkinson's disease

Table II - MDS Criteria for a Clinical Diagnosis of PD. Adapted from: Postuma et al., MDS clinical diagnostic criteria for Parkinson's disease (28)

The MDS criteria introduced two levels of certainty in the diagnosis: clinically established PD cannot present neither exclusion criteria nor “red flags” for alternative diagnosis, while clinically probable PD can present up to 2 red flags which must be counterbalanced by an equal number of supportive criteria. The former level (“clinically established”) aims to maximize specificity, while the latter aims for increased sensitivity. A validation study of the MDS criteria has shown excellent specificity (98.5%) and low sensitivity (59.3%) for the diagnosis of ‘clinically established PD’, whereas the diagnosis of ‘clinically probable PD’ had a specificity of 95% and a sensitivity of 96% (17).

Other diagnostic tests include:

- Dopamine transporter single-photon emission computed tomography (DaT SPECT): by showing decreased uptake of a radioactive tracer that binds to dopamine transporters in the basal ganglia, DaT SPECT can detect the presynaptic dopamine neuronal dysfunction observed in PD and other α-synucleinopathies. This exam has high sensitivity and specificity (98%–100%) for identifying nigrostriatal cell loss in parkinsonian patients.
- Genetic testing: not part of the routine diagnostic process, but should be considered for individuals with a specific suspicion for a possible genetic cause (i.e., family history, early onset, or specific clinical features, such as dystonia as a presenting symptom).
- Cerebrospinal fluid and blood tests measuring the levels of different α-syn protein types: currently presenting suboptimal sensitivities and specificities with no clinical use (14).

A new subtyping approach based on the predominant motor and non-motor features has been suggested, identifying the following phenotypes (15,30):

- Mild motor predominant: younger age at onset, lowest severity of both motor and non-motor symptoms, spared cognitive performance, slow progression, good medication response.
- Intermediate: intermediate age at onset (mean age at onset=65.4), values in the MDS-UPDRS (a scale used to evaluate both motor and non-motor features of PD) intermediate between the other two phenotypes, moderate-to-good response to treatment.

- Diffuse malignant: baseline severe motor symptoms accompanied by non-motor symptoms such as RBD, mild cognitive impairment and OH, worst scores in the MDS-UPDRS, worse medication response, prominent dopaminergic dysfunction on DaT SPECT, and rapid progression.

Parkinson Disease Subtype and Estimated Frequency	Disease Presentation	Response of Motor Symptoms to Dopaminergic Medication	Disease Progression
Mild motor predominant 49%-53%	• Young at onset • Mild motor symptoms	Good	Slow
Intermediate 35%-39%	• Intermediate age at onset • Moderate motor symptoms • Moderate nonmotor symptoms	Moderate to good	Moderate
Diffuse malignant 9%-16%	• Variable age at onset • Rapid eye movement sleep behavior disorder • Mild cognitive impairment • Orthostatic hypotension • Severe motor symptoms • Early gait problems	Resistant	Rapid

Table I – Proposed Parkinson Disease subtypes. Adapted from: Armstrong et al., Diagnosis and Treatment of Parkinson Disease (15)

1.2.5 Differential Diagnosis

Early diagnostic differentiation of PD from other α-synucleinopathies including atypical parkinsonisms might be challenging. Atypical parkinsonism is a broad term that applies to several neurodegenerative disorders with a parkinsonian syndrome as a prominent clinical feature but in which the full clinical spectrum, underlying pathology, progression, and prognosis may be different from PD (29).

The main differential diagnoses are:

- Vascular parkinsonism. Particularly in elderly patients, it is a common finding, accounting for an estimated 3-6% of parkinsonism cases (31). Ageing and vascular risk factors like hypertension, prior transient ischemic attacks (TIAs), and diabetes mellitus have been associated to this condition. Clinically, it is characterized by the predominance of parkinsonian symptoms at the lower limbs with impaired gait. Rest tremor is rare. While L-dopa response is often scarce, other symptoms of a brain vascular lesion, such as spasticity, hemiparesis, and pseudobulbar palsy, may be present. To confirm the diagnosis, structural brain imaging is crucial. DaT SCAN can

be useful in specific patients because it is typically normal in vascular parkinsonism. Nonetheless, a focal basal ganglia infarct can be the reason for an atypical scan result.

- Tremor disorders. Essential tremor (ET) is characterized by symmetric postural or kinetic hand tremor that can reach a frequency of up to 12 Hz, is rarely noticed at rest, and it is not accompanied by any parkinsonian symptoms or abnormal posture. About half of the patients show alcohol responsiveness, and head tremor may be observed (24).
- Dementia with Lewy bodies (DLB). These patients, typically elderly, experience noticeable daily fluctuations in alertness and cognition as well as vivid visual hallucinations. Additional characteristics that are frequently observed include dysautonomia, excessive susceptibility to neuroleptic medications, and RBD. There is considerable debate over whether DLB and PD could belong to the same disease because of their similar clinical and pathological findings. Current diagnostic criteria state that if the cognitive symptoms pre-date or develop within the first year of the emergence of parkinsonism, then the diagnosis is DLB. Should cognitive impairment develop in the context of established PD, then the diagnosis is PD dementia (PDD) (32).
- Atypical parkinsonisms [including MSA, Progressive Supranuclear Palsy (PSP), and Corticobasal syndrome (CBS)]. These conditions present with parkinsonism (rigidity and bradykinesia) but manifest with additional clinical features, including early autonomic dysfunction, early involvement of speech and gait, absence of rest tremor, poor or no response to L-dopa, and a more aggressive clinical course. L-dopa may only provide a modest improvement in the early stages.
    - MSA a combination of parkinsonian, cerebellar, and autonomic characteristics, leading to a subclassification in a predominant parkinsonian (MSA-p) or cerebellar (MSA-c) phenotype. When a patient exhibits the atypical parkinsonism symptoms mentioned above along with cerebellar signs and/or prominent autonomic dysfunction (typically OH or urinary disturbances), MSA can be clinically suspected. Pathologically, MSA is characterized by degeneration of the substantia nigra pars

compacta, striatum, cerebellum, and inferior olivary nuclei due to the characteristic α-syn glial cytoplasmic inclusions (GCIs). Imaging can be useful in discriminating PD and MSA. Structural imaging using magnetic resonance imaging (MRI) can reveal changes in the brainstem and basal ganglia which are supportive of MSA, including cerebellar and pontine atrophy, the “hot cross bun” sign, or a hypertense rim surrounding the putamen in T2-weighted sequences (24,33).

- PSP is characterized by slow ocular saccades, eyelid apraxia, and restricted vertical eye movements. Patients commonly experience early gait disturbance, falls, and neck hyperextension. Cognitive impairment and difficulties in speaking and swallowing may appear in later stages. Clinical predominance types are determined according to the MDS clinical diagnostic criteria for PSP (MDS-PSP criteria) (34) based on the combination of clinical features. These include early onset postural instability with vertical ocular motor dysfunction referred to as Richardson’s syndrome (PSP-RS), initial predominance of ocular motor dysfunction (PSP-OM), postural instability (PSP-PI), Parkinsonism resembling idiopathic PD (PSP-P), frontal lobe cognitive or behavioral presentations (PSP-F), including behavioral variant frontotemporal dementia (bvFTD), progressive gait freezing (PSP-PGF), corticobasal syndrome (PSP-CBS), primary lateral sclerosis (PSP-PLS), cerebellar ataxia (PSP-C), and speech/language disorders (PSP-SL). In midsagittal scans of the brain, MRI may show a distinctive atrophy of the midbrain with a relatively preserved pons (the so-called "hummingbird sign"). Pathologically, substantia nigra pars compacta, striatum, subthalamic nucleus, midline thalamic nuclei, and pallidum all exhibit degeneration along with neurofibrillary tangles and inclusions that stain for tau protein.
- CBS usually presents with asymmetric dystonia and clumsiness involving the upper limbs, associated with cortical sensory disturbances that can manifest as apraxia, agnosia, focal limb myoclonus, or alien limb phenomenon (where the limb assumes a

position in space without the patient being aware of the position or recognizing that the limb belongs to him/her). Dementia may occur at any stage of the disease. To diagnose this condition, both cortical and basal ganglia features must be present. Achromatic neuronal degeneration with tau deposits constitutes the most common pathological findings.

- Secondary parkinsonisms. Many primary conditions, such as the use of specific drugs, a stroke in the basal ganglia, a tumor, an infection, or exposure to toxins such as carbon monoxide or manganese can result in secondary parkinsonisms. Antipsychotics are the most common cause of drug-induced parkinsonism, particularly the "typical antipsychotics" including haloperidol and chlorpromazine. Other causes of drug-induced parkinsonism include anti-emetics (e.g., metoclopramide and domperidone), calcium channel blockers (e.g., flunarizine and cinnarizine), anti-epileptics (e.g., sodium valproate and phenytoin), and selective serotonin reuptake inhibitor anti-depressants (32,35).
- Other neurodegenerative diseases such as Wilson's disease, Huntington's disease, several forms of spinocerebellar ataxias (SCA) such as SCA2, SCA3 and SCA17, and disorders with brain iron accumulation such as pantothenate kinase (PANK)–associated neurodegeneration (formerly known as Hallervorden-Spatz disease) (21).

TABLE 427-2 Differential Diagnosis of Parkinsonism

Parkinson's Disease	Atypical Parkinsonism	Secondary Parkinsonism	Neurodegenerative Disorders and other forms of parkinsonism
Sporadic	Multiple-system atrophy (MSA)	Drug-induced	Wilson's disease
Genetic	Cerebellar type (MSA-c)	Tumor	Huntington's disease
Dementia with Lewy bodies	Parkinson type (MSA-p)	Infection	Neurodegeneration with brain iron accumulation
	Progressive supranuclear palsy	Vascular	SCA 3 (spinocerebellar ataxia)
	Parkinsonism	Normal-pressure hydrocephalus	Fragile X–associated ataxia-tremor-parkinsonism
	Richardson variant	Trauma	Prion disease
	Corticobasal Syndrome	Liver failure	X-linked Dystonia-parkinsonism
	Frontotemporal dementia	Toxins (e.g., carbon monoxide, manganese, MPTP, cyanide, hexane, methanol, carbon disulfide)	Alzheimer's disease with parkinsonism
			Dopa-Responsive Dystonia

Abbreviations: MPTP, 1-methyl-4-phenyl-1,2,5,6-tetrahydropyridine.

Table III – Differential Diagnosis of Parkinsonism. Adapted from: Harrison et al., Harrison's Principles of Internal Medicine (21)

1.2.6 Prognosis

The median survival after the diagnosis of PD is 9.1 years (95% CI: 7.4–10.9 years). PD has been associated to a higher risk of mortality (HR, 1.83; 95% CI, 1.47-2.26) (36). Aspiration pneumonia is the most frequent cause of death in PD patients (15). A post-mortem investigation revealing a close chronological link between the development of clinically meaningful dysphagia and a median survival period of less than two years further supports the importance of aspiration pneumonia as a factor in the increased mortality in PD (37).

1.2.7 Treatment

To date, despite the lack of disease modifying treatments that can clearly halt or cure the neuronal degeneration underlying PD, therapies offering significant symptom control are available (38). The three pillars for the management of PD are: medical therapy for both motor and non-motor symptoms, advanced or device-aided therapy and supportive care.

a) Medical treatment

Currently many different classes of drugs are available for the management of PD with the first choice being L-dihydroxyphenylalanine (L-dopa). The theoretical basis for the use of this substance lies in the fact that, although PD patients present decreased levels of striatal dopamine, the remaining nigral cells are still able to produce some dopamine by absorbing its precursor, L-dopa (38). Long-term use may lead to motor complications such as dyskinesias (uncontrollable twisting and hyperkinetic motions, which typically occur at peak dose), and extreme on-off motor fluctuations (39). Due to the short half-life of L-dopa and the erratic nature of both its gastrointestinal absorption and blood-brain barrier (BBB) transit, discontinuous drug distribution is the main contributing factor to motor fluctuations. Despite its effectiveness, L-dopa can cause adverse effects. Some of its side effects are due to L-dopa being converted to dopamine outside of the CNS by DOPA-decarboxylase. Therefore, L-dopa is administered along with peripheral inhibitors of aromatic amino acid decarboxylase (AADC), such as carbidopa or

benserazide, to stop peripheral dopamine metabolism and increase bioavailability, minimizing these side effects. These substances block the peripheral conversion of L-dopa to dopamine, but do not cross the BBB (39).

Dopamine agonists (DAs) (i.e., ropinirole, pramipexole and ritigotine) have a direct dopaminergic effect on striatal neurons, with less dyskinetic motor complications than L-dopa. Common side effects include OH, nausea and dizziness (38).

Entacapone, tolcapone, and opicapone (Catechol-O-methyltransferase inhibitors) can be used in combination with L-dopa+carbidopa/benserazide and have the ability of lengthening the half-life and increase the bioavailability of L-dopa. This is especially beneficial for patients who have developed motor fluctuations. The most common side effects include gastrointestinal and sleep disorders, as well as OH (14).

Monoamine oxidase B (MAO-B) inhibitors (selegiline, rasagiline, safinamide) function by inhibiting the enzymes responsible for dopamine metabolism, leading to an increase in the dopaminergic activity of the striatum. The most frequent side effects of MAO-B inhibitors are gastrointestinal; however, they are typically well tolerated (39).

Other medications, such as anticholinergic drugs, are used to treat PD via non-dopaminergic pathways. By acting as antagonists at cholinergic receptors, they might be helpful in patients with predominant tremor. Amantadine, originally developed as an antiviral medication, is now used as add on therapy in PD. Its pharmacological actions are both dopaminergic and glutamatergic, which account for its dual effect on parkinsonian signs and symptoms and L-dopa-induced dyskinesias. Furthermore, amantadine has additional and less well-defined pharmacological effects, including anticholinergic and serotonergic activity (39,40).

Regarding the management of non-motor symptoms, including neuropsychiatric symptoms, the DAs might have antidepressant efficacy, however usually additional treatment with selective serotonin reuptake inhibitors (SSRIs), serotonin and norepinephrine reuptake inhibitors (SNRIs) or tricyclic antidepressants (TCAs) is needed. These drugs, especially SSRIs, can also be used to treat anxiety,

as anxiety and depression often coexist. In case of psychosis, DAs should be reduced and, if this does not result in a sufficient improvement, a reduction of the L-dopa dosage should be considered. If none of these treatment-modifying strategies is beneficial, treatment with atypical antipsychotics (Quetiapine, Clozapine) is recommended. In case of dementia Rivastigmine, a cholinesterase inhibitor, is the only drug with proven efficacy.

Autonomic dysfunction can greatly impact PD patients' quality of life and should be promptly diagnosed and treated. In patients with OH, the non-pharmacological approach (sleeping in a head-up position, fragmentation of meals, increased water and salt intake, etc.) is crucial and can be implemented with pharmacological treatments including fludrocortisone and midodrine. Prokinetics and laxatives are commonly used for constipation. Urogenital dysfunction can be treated with anticholinergic drugs and Sildenafil, a phosphodiesterase 5 (PDE5) inhibitor (an enzyme that promotes breakdown of cGMP, which regulates blood flow), is useful for erectile dysfunction (ED) (15,41).

b) Advanced PD treatment

Deep brain stimulation (DBS) determines a chronic electrical stimulation of the brain using an implanted electrode. In the most widely used DBS system, an implantable pulse generator (IPG), which resembles a pacemaker and is positioned on the chest wall beneath the collarbone, is connected to a four-contact stimulating electrode through a subcutaneous wire (42). The main hypothesis states that electrical stimulation may cause inhibition of basal ganglia output structures, reducing basic neuronal firing and suppressing spontaneous neuronal activity (43). As stated by the EAN/MDS guidelines for the invasive treatment of Parkinson's Disease (44), lesional approaches such as radiosurgery, magnetic resonance imaging–guided focused ultrasound surgery and radiofrequency, pallidotomy, thalamotomy or lesioning of the subtalamic nucleus are not recommended or are to be offered only to eligible patients. On the other hand, DBS of the subthalamic nucleus (STN-DBS), DBS of the globus pallidum internum (GPi-DBS), L-Dopa/Carbidopa intestinal gel infusion and apomorphine infusion are all "non-lesional" approaches that can be offered to eligible patients due to their validated positive outcomes.

c) Supportive care

The management of axial and motor symptoms in PD patients is greatly aided by physical therapy (PT), which involves gait, posture, balance, physical capacity, and physical exercise. Moreover, several studies pointed out the benefits of aerobic exercise (26). Speech therapy can be introduced in order to improve voice and dysphagia in PD patients. Occupational therapy is also effective in improving daily life activities (45).

1.3 Multiple System Atrophy (MSA)

MSA is a sporadic, adult-onset neurodegenerative disorder characterized by autonomic failure and either parkinsonism (MSA-p) or a cerebellar syndrome (MSA-c), and an aggressive clinical course (21,46).

1.3.1 Epidemiology

The annual incidence of MSA is approximately 0.6 per 100 000, increasing to 3 per 100 000 in the population over 50 years old. The prevalence varies from 1 to 4 per 100 000 individuals (47). Regional and population-specific characteristics point to the possibility that environmental, genetic, and/or epigenetic variables might have a role in the pathogenesis of MSA. These findings are corroborated by reports of family aggregation of MSA in individuals with European and Japanese ancestry (46). The prevalence of MSA is slightly higher in men (1.3:1), with a mean onset age of 54 and a median survival of 7-9 years. At five and ten years after the onset of symptoms, the projected survival rates are 83.5 and 39.9%, respectively (48).

1.3.2 Neuropathology

Selective neurodegeneration and a distinct oligodendrogliopathy with argyrophilic GCIs are the neuropathological hallmarks of MSA. More than 20 years after their first description, GCIs or Papp-Lantos inclusions are currently universally recognized as indicators for the conclusive neuropathological diagnosis of MSA and are proposed to be key players in the pathophysiology of this condition.

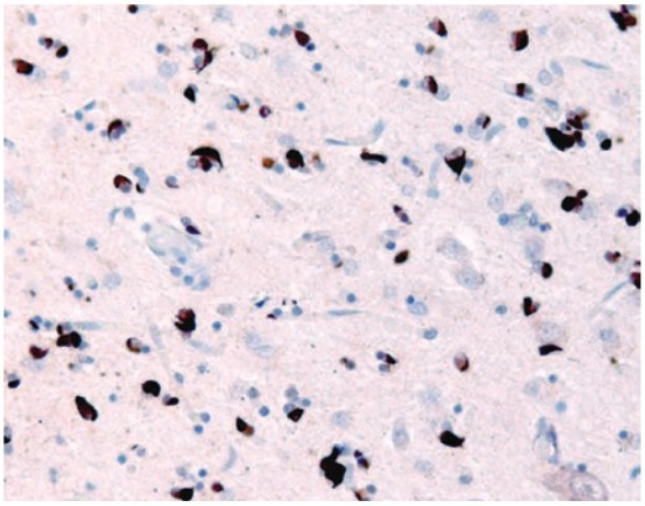

Fig.2 - MSA with numerous 'flame shaped'α-syn-containing inclusions within glia. Immunohistochemistry for α-syn. Adapted from: Hilton et al., Neurodegenerative Disorders (18)

From the neuropathological point of view, besides phosphorylated α-syn, ubiquitin, LRRK2 (leucin-rich repeat serine/threonine protein), and numerous other proteins have been detected inside GCIs (49). Other frequent pathological findings include reactive astrogliosis and activated microglia. There is evidence that implies that MSA is a primary oligodendrogliopathy, even if the underlying pathogenic mechanisms are still not completely understood. The relocalization of myelin stabilizer p25 into the oligodendroglial soma appears to occur before α-syn aggregation. Subsequently, oligodendrocytes enlarge and oligodendroglia abnormally takes up or overexpresses α-syn. As a result of the interaction between the two proteins, α-syn is phosphorylated and forms insoluble oligomers accumulating into GCIs. As the disease progresses, and as oligodendrocytes become increasingly dysfunctional, they release misfolded α-syn into the

extracellular space, which may then be taken up by nearby neurons to continue forming neuronal cytoplasmic inclusions (50). The striatonigral system experiences the greatest neuronal loss in MSA-p, whereas MSA-c presents predominant dysfunction in the olivopontocerebellar projections (46).

1.3.3 Clinical presentation

In 20 up to 75% of patients, MSA has a prodromal premotor phase that includes sexual dysfunction, urge incontinence or retention, OH, inspiratory stridor, and RBD. Patients present both motor and non-motor features.

Early and severe autonomic failure is a key feature of MSA. Neurogenic OH is caused by inadequate noradrenergic neurotransmission and decreased noradrenaline release from sympathetic vasomotor neurons. In addition to recurrent syncope, other signs and symptoms of OH are headache, trembling, dizziness, nausea, generalized weakness, and pain in the nuchal regions, frequently referred to as "coat hanger pain" and only felt when upright. The hypotensive side effects of L-dopa therapy, as well as fluid loss, infections, or physical deconditioning, may worsen OH (46). In patients diagnosed with MSA-p, orthostatic symptoms seemed to be more common (p-value=0.04). Moreover, only 68% of patients with a recorded drop in blood pressure of 30/15 mmHg or greater reported orthostatic symptoms, and only 27% experienced syncope. Urogenital dysfunction is common and included in the diagnostic criteria (51), with urge incontinence and incomplete bladder emptying, together with sexual dysfunction (especially ED in male patients) (52). Other features of autonomic failure include GI dysfunctions (i.e., constipation), pupillomotor abnormalities (i.e., spontaneous, gaze-evoked, or positional downbeat nystagmus), and vasomotor and thermoregulatory failure with diminished or absent sweating (hypohidrosis and anhidrosis). Respiratory disturbances are characteristic of MSA, with diurnal or nocturnal inspiratory stridor developing in as many as 50% of patients (50).

Depression negatively impacts quality of life in more than 40% of MSA patients, whereas other neuropsychiatric features seemed to be much less prevalent when compared with PD (52).

Motor features tend to appear in a later stage, with both extrapyramidal or cerebellar involvement. Parkinsonism, predominant in MSA-p, is characterized by rigidity, frequent falls, unstable posture, and action tremor with superimposed jerks. The motor presentation of MSA-c is dominated by cerebellar ataxia. Wide-based gait, uncoordinated limb movements, action tremor, and spontaneous, gaze-evoked, or positional downbeat nystagmus are all cerebellar features. Babinski sign, as well as generalized hyperreflexia, could be present. Advanced illness is distinguished by recurrent falls, dysphonia (voice-tone alterations), dysarthria (difficulty articulating words), drooling, and dysphagia (50).

1.3.4 Diagnosis

The most critical step in the assessment of a patient with suspected MSA is a thorough clinical evaluation, which includes comprehensive medical history, physical and neurological examination with specific focus on gait, coordination, and muscle tone (53). According to the "Second consensus statement on the diagnosis of multiple system atrophy" by Gilman et al. (54), there are currently three diagnostic categories: definite, probable and possible.

Definite diagnosis can be achieved only by neuropathologic findings of widespread CNS α-syn–positive GCIs (Papp–Lantos inclusions) along with neurodegenerative alterations in the striatonigral or the olivopontocerebellar regions.

The criteria for probable MSA are as follows: a sporadic, progressive, adult (>30 years old)-onset disease characterized by

- Autonomic failure involving urinary incontinence (inability to control the release of urine from the bladder, with ED in males) or an orthostatic decrease of blood pressure within 3 min of standing by at least 30 mmHg systolic or 15 mmHg diastolic and
- Poorly L-dopa-responsive parkinsonism (bradykinesia with rigidity, tremor, or postural instability) or cerebellar syndrome (gait ataxia with cerebellar dysarthria, limb ataxia, or cerebellar oculomotor dysfunction). Of course, patients with predominantly parkinsonian features should be

categorized MSA-p, while patients with predominantly cerebellar ataxia should be categorized MSA-c.

Criteria for possible MSA include: a sporadic, progressive, adult (>30 years old)-onset disease characterized by

- Parkinsonism or a cerebellar syndrome
- at least one feature suggesting autonomic dysfunction (i.e., urinary urgency, frequency or incomplete bladder emptying, ED in males, or significant orthostatic blood pressure decline that does not meet the level required in probable MSA)
- at least one of the additional features shown in the following table.

Possible MSA-P or MSA-C
• Babinski sign with hyperreflexia
• Stridor
Possible MSA-P
• Rapidly progressive parkinsonism
• Poor response to levodopa
• Postural instability within 3 y of motor onset
• Gait ataxia, cerebellar dysarthria, limb ataxia, or cerebellar oculomotor dysfunction
• Dysphagia within 5 y of motor onset
• Atrophy on MRI of putamen, middle cerebellar peduncle, pons, or cerebellum
• Hypometabolism on FDG-PET in putamen, brainstem, or cerebellum
Possible MSA-C
• Parkinsonism (bradykinesia and rigidity)
• Atrophy on MRI of putamen, middle cerebellar peduncle, or pons
• Hypometabolism on FDG-PET in putamen
• Presynaptic nigrostriatal dopaminergic denervation on SPECT or PET

MSA = multiple system atrophy; MSA-P = MSA with predominant parkinsonism; MSA-C = MSA with predominant cerebellar ataxia; FDG = [^{18}F]fluorodeoxyglucose.

Table IV – Additional features of possible MSA. Adapted from: Gilman et al., Second consensus statement on the diagnosis of multiple system atrophy (54)

Imaging criteria are included in consensus guidelines for the diagnosis of potential MSA. These include the presence of atrophy of the putamen, middle cerebellar peduncle, pons or cerebellum in brain MRI; the "hot cross bun" sign, which is a cruciform hypointensity in the pons, and the "putaminal slit" sign, a hyperintense signal in the dorsolateral margin of the putamen, have a strong positive predictive

value for the diagnosis of MSA. Putamen, brainstem or cerebellum hypometabolism on brain fluorodeoxyglucose (FDG) positron emission tomography (PET), as well as dopaminergic denervation on PET or SPECT are also present among the additional diagnostic features (53).

Supporting features include head–neck dystonia, disproportionate antecollis (or dropped head sign: a significant forward flexion of the head and neck), axial deformities such as camptocormia or Pisa syndrome, contractures of the hands or feet, inspiratory sighs, severe dysphonia, severe dysarthria, new or increased snoring, cold hands and feet, emotional incontinence (pathologic laughter or crying), jerky, myoclonic postural or action tremor. Among the red flags (warranting a different diagnosis than MSA), we can include: classic "pill-rolling" rest tremor, neuropathy, hallucinations not drug-induced, onset after 75 years of age, family history of ataxia or parkinsonism, dementia, white-matter lesions compatible with multiple sclerosis (54).

There are many ancillary tests that can assist in the diagnosis and should be performed when possible. For example, olfactory testing may discriminate between PD and MSA with extremely high specificity and modest sensitivity; autonomic testing, neuroimaging and urological evaluation can also help in the differential diagnosis. However, the diagnosis of probable or possible MSA is based on clinical history and the neurological exam and can only be confirmed pathologically post mortem (53).

1.3.5 Differential diagnosis

In a 2015 study by Koga et al. (55), patients with a clinical antemortem diagnosis of MSA, underwent autopsy and pathological validation. However, the diagnostic accuracy was only 62%, with the most common misdiagnosis being DLB (37%), followed by PSP (29%), PD (15%), and other disorders (18%).

Many disorders are included in the differential diagnosis of MSA. The most frequent misdiagnosis is PD, especially when evaluating patients with MSA-p. When motor signs are subtle with predominant autonomic presentation, a misdiagnosis with pure autonomic failure (PAF) can occur. However, the majority

of MSA cases that begin with autonomic failure tend to develop additional neurological symptoms within 5 years. PSP and CBS are also part the differential diagnosis process of MSA-p, as does (even if rarely) primary lateral sclerosis (PLS) or the PLS presentation of amyotrophic lateral sclerosis (ALS). As for MSA-c, major differential diagnosis is with SCA 2 and 3, which can present with a combination of cerebellar and parkinsonian characteristics, even though a positive family history may help in the diagnosis (56).

1.3.6 Prognosis

A continuous deterioration of both motor and non-motor symptoms over an average of 10 years is typical of MSA. The median survival in patients with MSA has been reported around 6-10 years after the onset (50). It is noteworthy that while some MSA patients have significantly longer disease durations—up to 20 years—others have survival as low as 2 years, partially depending on the magnitude and duration of L-dopa response. Early autonomic failure has been observed in patients with faster disease progression and lower survival, with early stridor being a significant risk factor for reduced survival (57). In MSA, infections including bronchopneumonia and urosepsis are frequent causes of death, together with acute bilateral vocal cord paralysis or abrupt interruption of the brain-stem cardiorespiratory drive (50).

1.3.7 Treatment

No disease-modifying treatments are currently available. Except for one, all randomized, controlled neuroprotection trials were unsuccessful (57). The only successful study to date was one that reported positive effects of intravenous and intraarterial injections of mesenchymal stem cell (MSCs) on the progression of UMSARS scores. The primary target for the creation of potential neuroprotective therapies for MSA is presently α-syn. In this regard, a phase 1 trial using active anti-synuclein immunization was performed in 30 MSA patients. It is extremely likely

that further methods for targeting α-syn (e.g., passive immunization, antiaggregation) will be used in the future.

First line treatment for parkinsonism in MSA patients is L-dopa and in general protocols used in patients with PD including DAs and MAO-B inhibitors such as safinamide. The most effective treatment for cerebellar ataxia is still physiotherapy. Clonazepam, vitamin E, propanolol, baclofen, or amantadine have all demonstrated partial and transitory efficacy when used off-label. In a small open-label experiment with only 9 MSA-c patients, buspirone (off-label) seemed to improve upper-limb ataxia (58).

Regarding non-motor symptoms, milder manifestations of OH may be managed with non-pharamacological approaches (e.g., compressive manoeuvres and devices, changes in diet and activities, etc.). However, patients experiencing syncope will need to be treated pharmacologically, with the most effective medication being midodrine.

Patients with neurogenic bladder should undergo regular urologic follow-up including routine urinalysis to rule out urinary tract infections (UTIs). Antimuscarinic medications can be used to treat urinary urge incontinence due to detrusor overactivity; those refractory to medication may try botulinum toxin injections in the detrusor muscle. Nycturia can be ameliorated by a head-up tilt during sleep and bedtime administration of desmopressin. First-line treatment for urine retention with postvoid residual volumes greater than 100 ml is clean intermittent self-catheterization. Sildenafil can help men with ED, but worsening of OH is a known side effect (50,59).

1.4 New biomarkers in α-synucleinopathies

The availability of accurate and easily accessible biomarkers providing an early diagnosis is still an unmet need, particularly in synucleinopathies, where the prompt identification of the disease, possibly prior to the onset of motor and cognitive symptoms, and an accurate differential diagnosis are key. Moreover, in light of the recent availability of potentially disease modifying therapies, the early identification of eligible patients is crucial (60).

1.4.1 Fluid biomarkers

α-syn has been proposed as a possible biomarker in PD, due to the fact that it is easily secreted into extracellular spaces and can be found in different forms (monomeric and seeding-competent aggregated forms) in body fluids such as CSF, blood components, saliva, and tears as well as in peripheral tissues (such as skin, oesophagus, and colon). Different techniques have been developed in order to provide a non-invasive detection and monitoring of α-syn in biological fluids and tissues (61). Protein misfolding assays, which were originally used to amplify and identify misfolded prion protein associated to prion disorders, have gained increasing interest in the context of α-synucleinopathies. These assays, originally designed adapting the idea of DNA amplification by polymerase chain reaction, include the protein misfolding cyclic amplification (PMCA) and the real-time quaking-induced conversion (RT-QuIC) assays, which share a similar conceptual basis but differ in technical aspects, such as substrate, buffer, pH, and shaking settings. These methods are especially noteworthy because they simulate in a lab the seeding and misfolding of α-syn, which is the main mechanism underlying the propagation and transmission of misfolded proteins from cell to cell. The basic idea behind these methods is that a template expands at the expense of a substrate in a cyclic reaction. Each cycle consists of two phases: the first phase involves incubating a sample containing a small number of misfolded oligomers and an excess of monomeric protein in order to stimulate the growth of polymers. The sample is then subjected to a mechanical force to break down the polymers and increase the number of seeds in the second phase. Fluorescent dyes (thioflavinT, ThT) are used to visualize the reaction, which results in an exponential increase in the number of seeds after each cycle (60,62). This technique can be applied in all biological fluids, but so far studies focused particularly on the detection of α-syn in blood and CSF.

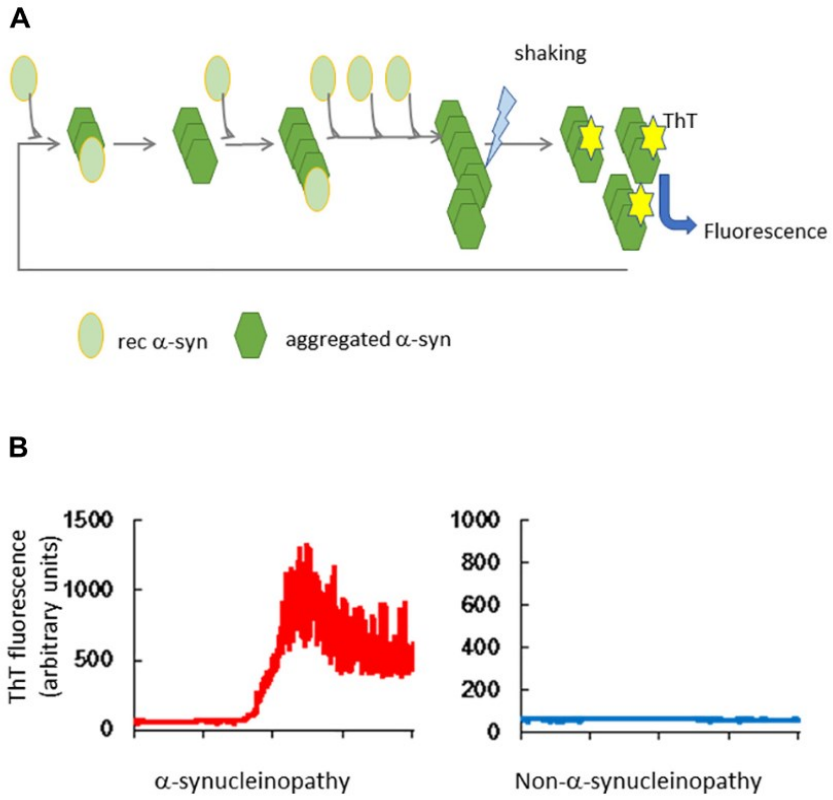

Fig.3 - (A) By repeatedly shaking and incubating, aggregated α-syn transforms rec α-syn into the aberrant structure, which creates amyloid. Thioflavin T (ThT) binds to the amyloid's β-sheet structure and emits fluorescence. (B) The left panel displays the results from a brain homogenate from a patient with synucleinopathy, while the right a healthy control. Adapted from: Nakagaki et al., Development of α-Synuclein Real-Time Quaking-Induced Conversion as a Diagnostic Method for α-Synucleinopathies (63)

Being largely expressed outside the CNS, α-syn may be also detected in blood. However, haemolysis and red blood cell (RBC) contamination have a significant impact on its blood levels, with RBCs accounting for the majority (>99%) of the α-syn in blood. It is likely that even a small amount of RBC contamination might cause a significant increase in its levels in serum or plasma. Therefore, research has been focusing on the oligomeric and phosphorylated species showing encouraging results (64).

CSF total α-syn (t-α-syn) concentrations have showed a small reduction in PD patients compared to healthy and disease controls, as determined by a variety of studies and meta-analyses. The efficacy of CSF t-α-syn in differentiating PD from the atypical parkinsonisms is, however, limited because lower α-syn concentrations were also documented in other disorders that are not related to α-

syn misfolding, such as CBS and vascular parkinsonism. As a result, pathogenic species of α-syn, such as S129-phosphorylated (p-α-syn), oligomeric (o-α-syn), and proaggregating forms, have been examined as potential diagnostic biomarkers. The levels of p- and o-syn in the CSF were observed to be higher in PD than in controls, however their diagnostic efficacy is insufficient for use in clinical practice when taken individually (7). In fact, one study reported t-α-syn had a sensitivity of 59% and a specificity of 80%, while o-α-syn showed a sensitivity of 89% and a specificity of 48% (65). Moreover, these biomarkers are not yet helpful in effectively supporting the differential diagnosis of atypical parkinsonisms.

A few studies (66,67) have also focused on β-syn as a possible fluid biomarker for neurological diseases. The first quantitative data on CSF β-syn concentrations in patients with α-synucleinopathies, obtained with an innovative mass spectrometry method, were published in 2016 (68). No statistically significant difference was found between PD patients and controls, although PD with dementia (PDD) and DLB patients had slightly increased levels of β-syn, which rose substantially when the ratio of β-syn to α-syn was considered, suggesting a possible supporting role of β-syn in the identification of cognitive impairment in α-synucleinopathies (7).

Several studies recently focused on neurofilament subunits (particularly the light neurofilaments NfL) released in the CNS interstitial space after axonal damage or degeneration, as potential biomarkers in neurodegenerative disorders. Therefore, in the last ten years, ultrasensitive techniques (i.e., single molecule array) have been developed in order to obtain an accurate quantification of NfL in biological fluids, namely CSF and blood. CSF NfL concentrations have been shown to be higher in patients with atypical parkinsonisms compared to those with PD, with excellent accuracies in discriminating PD from PSP (AUC 0.97, sensitivity 93%, specificity 95%), MSA (AUC 0.95, sensitivity 89%, specificity 93%), and CBS (AUC 0.96, sensitivity 100%, specificity 93%). Because blood NfL has a diagnostic accuracy similar to CSF NfL, it might represent a valid biomarker in the differential diagnosis between PD and atypical parkinsonisms (64).

1.4.2 Skin biopsy

Previous studies showed the presence of α-syn deposits within many structures of the PNS such as pharyngeal nerves, nerves of the submandibular and minor salivary glands and nerves and ganglia of the enteric nervous system and dermal nerve fibers (69). Among these, skin biopsies have been identified as promising and easily accessible procedures, supported by data from a meta-analysis by Tsukita et al. (70), observing that the diagnostic accuracy of immunohistochemical (IHC) detection of p-α-syn in dermal nerve fibers was higher when compared with the examination of other tissues. The morphological appearance of p-α-syn deposits in the skin did not differ from Lewy neurites found in the substantia nigra. As described in literature, they have a threadlike appearance and occasionally show uneven varicosities. The deposits were primarily discovered in autonomic fibers. Therefore, the inclusion of autonomic structures like sweat glands, vessels, or erector pili muscles in the skin section has a significant impact on the ability to detect α-syn in skin biopsies. Not only the deposits were equally prevalent in individuals in the early and late stages of the disorder (showing that cutaneous nerve fibers are involved in PD at an early stage), (69) but a significant correlation was found between α-syn deposition in autonomic small fibers and the severity of motor and autonomic symptoms. Moreover, there were consistent correlations between the deposition of α-syn and RBD, dopamine transporter deficiency, and olfactory impairment. According to these data, cutaneous p-α-syn is able to identify prodromal PD (71). Moreover, skin biopsies disclosed an important role in the differential diagnosis of α-synucleinopathies. In a study by Donadio et al. (72) it was observed that all 21 of PD patients had α-syn aggregation in the skin samples, as opposed to the 20 patients with parkinsonism (i.e., vascular parkinsonism, tauopathies, and pathogenic Parkin mutations). It was also described that in MSA aberrant deposits are mostly found in the somatic terminals, whereas in PD they are found in the autonomic fibers, showing a potential role in the differential diagnosis (73).

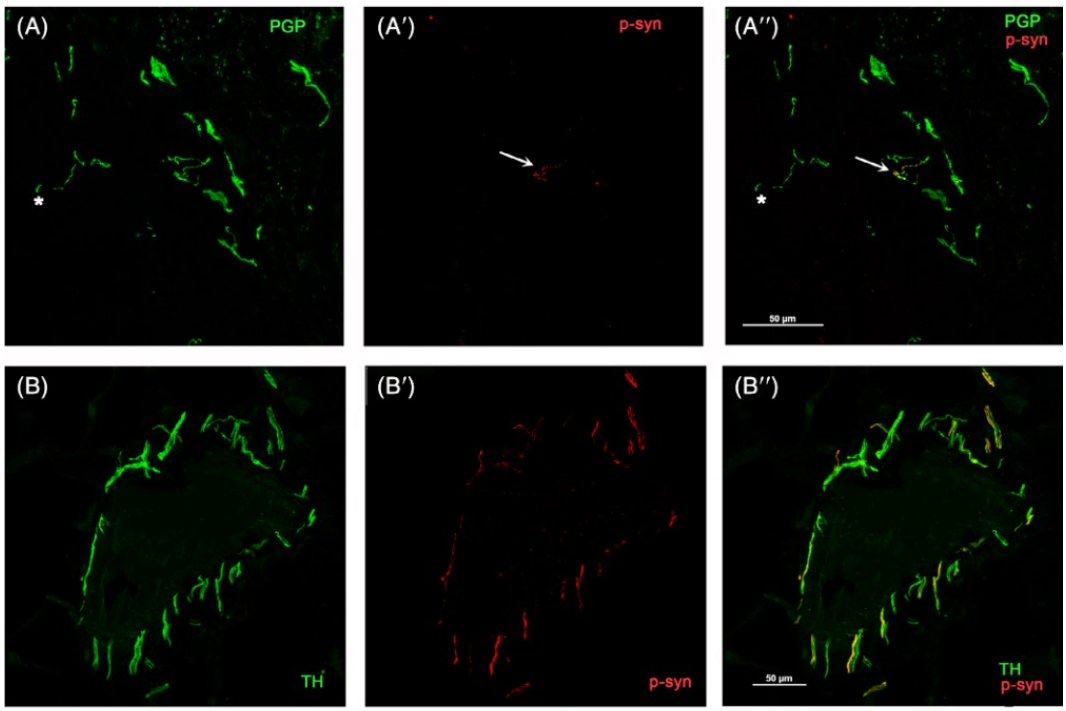

Fig.4 - Confocal microscope study of p-syn deposition in MSA-p and PD with OH. (A–A"). In MSA-p, abnormal p-syn deposits were found in the somatic nerves of subepidermal plexi in the superficial dermis. These plexi are identified by pan-neuronal marker protein gene product (PGP)(A). p-syn was depicted by staining the phosphorylation at Ser 129 (A'). Abnormal p-syn deposits were neuritic inclusions(A"). (B–B") By contrast, abnormal α-syn aggregates were found in the autonomic fibers of the deep dermis in PD+OH. Adrenergic nerve fibers were identified by tyrosine-hydroxylase (TH) (B). Most of the TH immunoreactive fibers showed positive p-syn (B') as neuritic inclusions demonstrated by the merged image (B"). Adapted from: Donadio et al., Skin Biopsy May Help to Distinguish Multiple System Atrophy Parkinsonism from Parkinson's Disease With Orthostatic Hypotension (73)

RT-QuIC can also be used on skin samples and it was validated in a dual center comparison study by Kuzkina et al. (74). This study found that not only α-syn seeding activity detected by RT-QuIC is increased in skin biopsies from PD patients (with an 88.9% diagnostic accuracy; sensitivity 90.9%, specificity 86.7%), but that it also correlates with disease duration and stage, making it a very valuable and promising method.

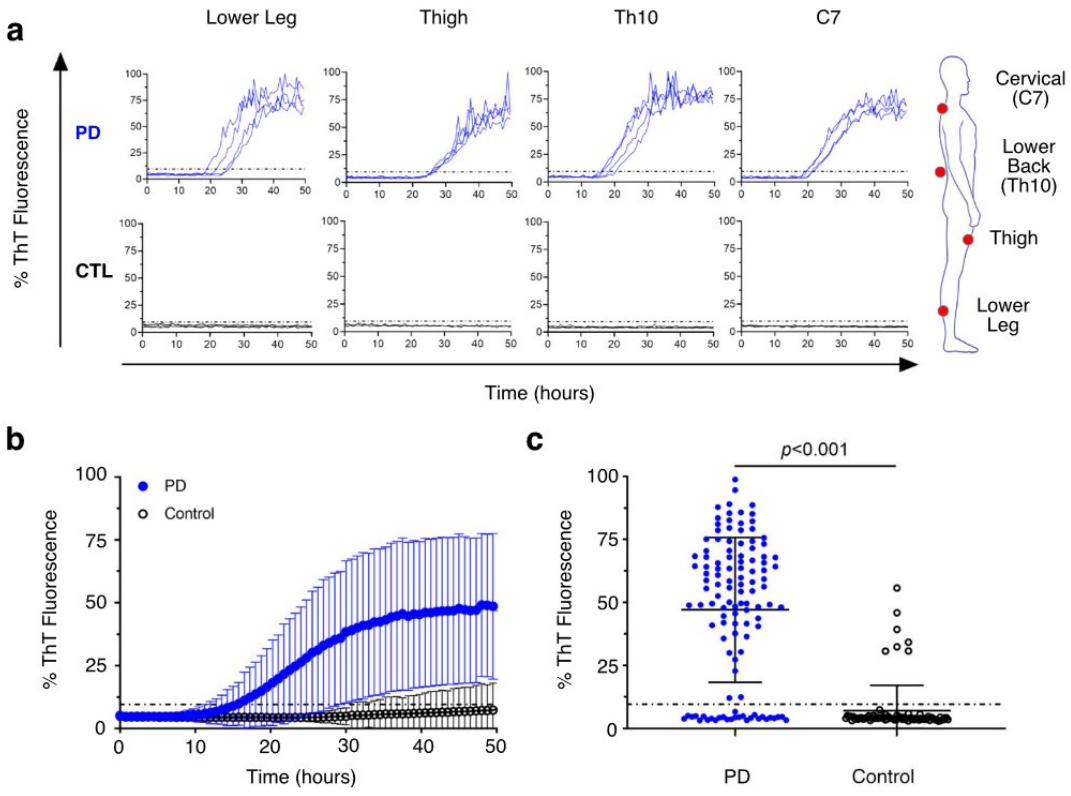

Fig.5 – a) α-Syn RT-QuIC assay of multiple skin biopsies from a PD patient and a control subject at the level of C7 (neck), Th10 (lower back), thigh, and lower leg. Individual ThT fluorescence responses over time for each skin sample tested. b) Cumulative results of blinded testing of all skin biopsies. Mean values (±SD) of percentage of ThT fluorescence of all biopsies are clearly increased in PD patients. c) Scatter graph of final percentage of ThT fluorescence intensities (50 h) for all individual biopsies. Average ThT fluorescence intensities of skin biopsies from PD patients are significantly higher ($p < 0.001$) than those from control subjects. Adapted form: Kuzkina et al., Diagnostic value of skin RT-QuIC in Parkinson's disease: a two-laboratory study (74)

1.4.3 Optical Coherence Tomography

Optical Coherence Tomography (OCT) is a diagnostic technique providing high-resolution in vivo cross-sectional imaging of the retina, based on a concept known as inferometry (75). Due to its easy accessibility, non-invasivity and to the possibility of repeating the test along the follow-up of the patients, this test has been proposed as a possible complementary tool in the early diagnosis of different neurological disorders such as multiple sclerosis (MS) and several neurodegenerative diseases. OCT provides quantitative anatomical data and is

associated with low variability for repeated measurements, low intra- and inter-individual variability, and low variability across multiple centres utilizing the same equipment.

The retina is approximately 0.5 mm thick and lines the back of the eye. The optic nerve contains the ganglion cell axons running to the brain and incoming blood vessels. The ganglion cells (the output neurons of the retina) lie innermost closest to the lens and front of the eye, and the photosensors (the rods and cones) lie outermost in the retina (76). The retina has 10 distinct layers. From closest to farthest from the vitreous body:

1. Inner limiting membrane (ILM)
2. Retinal nerve fibre layer (RNFL)
3. Ganglion cell layer (GCL)
4. Inner plexiform layer (IPL)
5. Inner nuclear layer (INL)
6. Outer plexiform layer (OPL)
7. Outer nuclear layer (ONL)
8. External limiting membrane (ELM)
9. Photoreceptor layer (PR)
10. Retinal pigment epithelium (RPE)

The retina and optic nerve extend from the diencephalon during their embryonic development. Thus, both are part of the CNS. The optic nerve (ON), similarly to all fiber tracts in the CNS, is covered with oligodendrocyte-produced myelin and is sheathed by all three meningeal layers. However, the similarities with the CNS do not stop at the neural structure. Like the CNS, the eye has a unique relationship with the immune system that involves specialized barriers, such as the inner blood-retinal barrier, the retinal analog of the BBB (77). Since the changes of the retinal structure and microvasculature are seemingly correlated with neurodegenerative and cerebrovascular lesions (i.e., AD, MS, stroke), the retina may serve as an effective “window” to the brain (78). The CNS is usually difficult and costly to assess, therefore retinal imaging could provide a meaningful and low-cost tool in the early detection of neurological diseases. Moreover, since the retina's axons of the RCSs are nonmyelinated, the RNFL can be used to easily observe processes like neurodegeneration, neuroprotection, and neurorepair (77).

Several studies (79–81) showed a reduced dopamine concentration in the amacrine cells of the retina in PD patients, eventually leading to the thinning of the RGCs layer. Since these cells control receptive regions of the RGCs involved with colour vision and spatial contrast sensitivity, these findings may possibly explain the visual symptoms of the disease (82). Moreover, α-syn has been identified in the inner retina of PD patients. A meta-analysis of time domain (TD)-OCT and spectral domain (SD)-OCT imaging (83) showed that the peri-papillary RNFL (pRNFL) is thinner in PD patients compared to controls. When compared to healthy controls (HCs), studies showed that the perifoveal regions present a reduced inner retinal layer (IRL; defined as ILM + RNFL + GCL + IPL + INL) in PD patients (84). Moreover, retinal thinning in PD seems to mirror disease progression. In the prodromal phase and early-stages, atrophy of the ganglion cell–inner plexiform layer (GCIPL) complex is detected in the parafoveal region of the macula; in middle-stage PD, in addition to parafoveal GCIPL atrophy, atrophy of the temporal sector of the pRNFL is identified; in advanced-stage PD, a greater degree of retinal damage is observed, with global atrophy of the entire macular GCIPL and the pRNFL (85).

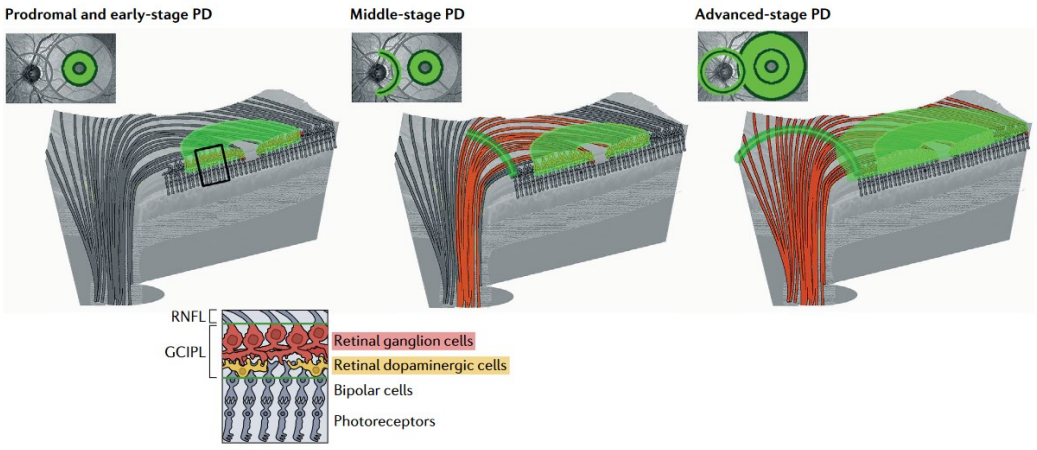

Fig.6 - Proposed retinal changes in PD identified by OCT. Adapted from: Lee et al., Multimodal brain and retinal imaging of dopaminergic degeneration in Parkinson disease (85)

In ophthalmological evaluations, different ocular dysfunctions have been identified and documented in individuals with CNS disorders such as MS, AD, and strokes. Ocular symptoms (including irregularities in ocular motility, visual loss, alterations in contrast sensitivity, and deficiencies in colour vision) frequently appear before neurological symptoms in many of these conditions, suggesting that

the ophthalmological examination may be helpful in the context of an early diagnosis of different neurodegenerative disorders (78).

Moreover, vascular dysfunction has been recognized as an associated factor in PD along with neurodegeneration. A study by Kwapong et al. (86) using OCT-angiography showed that PD patients present lower retinal microvascular density. Their results indicated that, when compared to HCs, the retinal capillary densities were significantly lower in the early stages of PD, indicating that retinal capillary impairment occurs before the appearance of clinically evident motor deficits. Baseline RNFL thickness was also associated with cognitive functions; in particular, patients with the thinnest baseline RNFL had significant impairment of global cognition, executive functions, and delayed memory. Moreover, these patients displayed a quicker deterioration in cognitive function. These findings suggest that OCT could also be used as a predictive biomarker for cognitive deterioration in PD patients (87).

Lee et al. (85) suggested that the combination of nigral MRI and retinal OCT may enhance diagnostic performance, offer data on both disease progression and prognosis and is a promising strategy for future imaging biomarker development in PD. Also, research focusing on the connection between degenerative processes in the substantia nigra and the retina may shed new light on the pathophysiology of PD.

pRNFL and, to a lesser extent, macular GCL complex atrophy have been observed in recent studies on MSA patients (88,89). However, patients with MSA rarely report visual complaints. In fact, if MSA patients report eye-related symptoms, these are usually caused by efferent (motor) visual system abnormalities, such as blepharospasm, blurry vision, or diplopia. Meta-analysis results (90) demonstrated significant thinning in all RNFL quadrants, except for the temporal RNFL quadrant, where MSA and controls showed similar thickness. This unique pattern of retinal damage suggests that MSA patients have preferential loss of large myelinated optic nerve axons like those originating from the magnocellular pathway (M-cells), which require higher support from oligodendrocytes and are not essential for visual acuity. Patients with MSA appear to experience retinal damage in a pattern that is specifically different from those with PD. While the inferior, superior, and nasal RNFL sectors are more impacted

in patients with MSA, the temporal RNFL sectors and internal retinal layers (IRL) [i.e., macular ganglion cell layer complex (mGCC), defined as IPL+GCL+RNFL] at the parafoveal area show greater atrophy in PD. Differences in the preferential damage of P-cells or M-cells could account for these disparities between PD and MSA. In PD patients, P-cells that are predominant in the central macular region with their axons projecting to the temporal region of the retinal nerve fiber layer are the most affected. They are closely related to colour discrimination, visual acuity, central visual field sensitivity, and contrast sensitivity for high spatial frequencies.

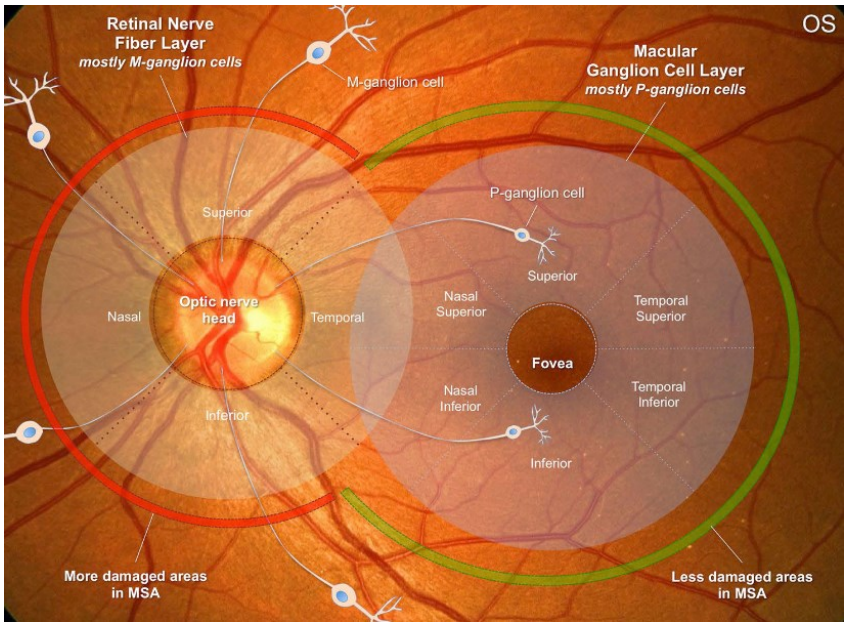

Fig.7 - Main findings in MSA patients. Adapted from: Mendoza-Santiesteban et al., The Retina in Multiple System Atrophy: Systematic Review and Meta-Analysis (88)

OCT has also been considered as a possible disease progression biomarker as it was demonstrated that pRNFL thinning correlates with greater disease duration and disease severity (UMSARS). It was also concluded that RNFL thickness by high definition-OCT meets several criteria as a potential new imaging endpoint for neuroprotection studies in MSA, including reproducibility, compliance, association with clinical observations, and sensitivity to changes over time (88).

SD-OCT also allows the identification of unique features inside the retinal layers in several retinal and neuro-ophthalmologic conditions (i.e., MS), namely hyperreflective intraretinal foci (HRF). These are hyperreflective, small (<30 µm) and round lesions that can be observed in every retinal layer (91). The underlying pathology is still unclear. Different hypotheses have been proposed, including lipid

extravasation in diabetic macular oedema (DMO) (92), degenerated photoreceptor cells (93), and migrating retinal pigment epithelial cells (94). However, one of the most accredited hypotheses suggests that HRF are constituted by clusters of activated and proliferating microglia (95). Microglia, the CNS-resident antigen-presenting cells, is increasingly recognized as a key player in the pathogenesis of inflammatory and neurodegenerative diseases (96). In PD, α-syn oligomers stimulate microglial cells, which respond by producing factors that are thought to be neurotoxic (97). Similarly, in MSA the abnormal extracellular presence of α-syn can be sensed and internalized by glial cells, leading to a cascade of reactive gliosis, secretion of pro-inflammatory cytokines and subsequent cell recruitment (98). This explains the typical MSA histopathology findings including myelin degeneration with astrogliosis and microglial activation (99). In MS, a neuroinflammatory disease, autoreactive peripherally activated T cells trigger an inflammatory cascade leading to the activation of resident CNS glial cells (such as microglia), which results in persistent inflammation even in absence of further infiltration of exogenous inflammatory cells (100). In a recent study, Pengo et al. (95) found an association between HRF counting and cortical pathology in MS and thus proposed its use as a candidate prognostic biomarker in the disease. To date, no studies on the correlation between HRF counting and MSA or PD have been published, however it appears to be a promising biomarker in neurodegenerative diseases as well.

In light of all these findings, growing interest has been shown in defining the role of OCT as a non-invasive technique able to provide reliable markers for the early diagnosis of PD.

2. Aim of the study

The aim of this study is to define the possible role of OCT and skin biopsy in the early diagnosis and follow-up of PD and MSA.

The primary goal is to investigate specific OCT and skin biopsy patterns in each disorder, in order to identify possible biomarkers specific for the diseases. Both OCT and skin biopsy will also be assessed as possible tools in the differential diagnosis of α-synucleinopathies.

Moreover, the presence of possible correlations between the OCT and skin biopsy data and the clinical and autonomic data from both PD and MSA patients will also be evaluated.

3. Materials and methods

3.1 Population

Patients referred to the Movement Disorder Unit in the Neurological Clinic of the University Hospital of Padova between 2019 and 2023 and diagnosed with either PD or MSA were considered.

The diagnosis of PD was made according to the 2015 International Parkinson and Movement Disorder Society (MDS) criteria (28), which are based on a clinical neurological examination demonstrating a parkinsonian syndrome (bradykinesia + rest tremor and/or rigidity) as well as the use of supportive and excluding characteristics. In a subgroup of patients, the clinical diagnosis was supported by the execution of DaT-scan.

The diagnosis of MSA was made according to the 2008 criteria of the Second consensus statement on the diagnosis of multiple system atrophy (54), which rely on clinical examination (mainly parkinsonism and/or cerebellar involvement, along with autonomic dysfunction) and can be supported by imaging or nuclear medicine tests.

The control group consists of healthy sex and age matched subjects. Controls were defined as probands without a history of parkinsonism or MSA and showing no neurological signs.

3.2 Clinical evaluation

All patients underwent standard neurological examination and were assessed using validated rating scales in order to determine disease severity and dysautonomia.

- MDS-Unified Parkinson's Disease Rating Scale (MDS-UPDRS)
  The validated MDS-UPDRS scale (101) was used to evaluate various aspects of Parkinson’s disease including non-motor and motor

experiences of daily living and motor complications. It is a useful tool in order to determine both disease severity and progression. In 2001, the Movement Disorder Society (MDS) sponsored a critique of the Unified Parkinson's Disease Rating Scale (UPDRS), which was originally developed in 1987 and was the most used clinical rating scale for Parkinson's disease. The MDS-UPDRS uses the same four-part format as the original UPDRS, with scores that can be added together to generate a total or be evaluated separately. The full revised version contains 50 questions, divided across Part I (13), Part II (13), Part III (18), and Part IV (6). The MDS-UPDRS part I is called "Non-motor Experiences of Daily Living". The questions were separated into simple ones that were thought to be better suited for a patient/caregiver questionnaire (sleep, staying awake, pain and abnormal sensory sensations, urinary function, constipation, lightheadedness on standing, and fatigue) and complex ones that require medical probing to obtain answers (cognitive impairment, hallucinations, depressed mood, anxious mood, apathy, and dopamine dysregulation). To create a conceptual parallel with Part I, the new Part II has been renamed "Motor Experiences of Daily Living" and it is to be completed by the patient or caregiver. It investigates, for example, the impact of the disease on daily tasks such as eating, writing, personal hygiene, and speech, walking and balance impairment. Part III is still designated as "Motor Examination," to be completed by the rater; it includes speech, rigidity, tremor and gait evaluation and other tests such as finger and toe tapping and leg agility. Part IV is limited to "Motor Complications" (dyskinesias and motor fluctuations). Disability or impairment is scored for each question on a scale from 0 to 4, where: 0=normal, 1=slight (low frequency or intensity that causes no impact on function), 2=mild (frequency or intensity sufficient to cause a modest impact on function), 3=moderate (symptoms/signs sufficiently frequent or intense to impact considerably, but not prevent function), and 4=severe (prevent function).

- Unified Multiple System Atrophy Rating Scale (UMSARS)

  In 2001, the European MSA Study Group (EMSA-SG) organized a task force with the specific goal of developing and validating a novel Unified MSA Rating Scale (UMSARS) (51). UMSARS rates functional impairment independent of underlying motor disorder, which can be parkinsonian or cerebellar or both and it introduces a five-point global disability scale analogous to the Hoehn & Yahr (H&Y) scale used for PD. Part I (12 items) includes a historical review of disease-related impairments, such as activities related to motor disability and four items related to autonomic dysfunction. Part II (14 items) consists of the motor examination, where most of the items (e.g., speech, finger taps, leg agility, rapid alternating movements of the hands) measure the functional impairment of selected complex movements, and only a few items directly refer to specific parkinsonian (tremor at rest) or cerebellar (ocular motor dysfunction, heel–shin test) features. Moreover, in contrast to the UPDRS, only the worst limb is assessed in the limb motor examination section of the UMSARS-II. For UMSARS-I and UMSARS-II, the maximum scores are 48 and 56 points, respectively. Part III investigates the main autonomic feature of MSA (i.e., OH). Each item receives a score that ranges from 0 (no impairment) to 4 (severe impairment). Lastly, part IV includes a global disability scale that goes from 0 (completely independent) to 5 (totally dependent and helpless; bedridden) based on disease severity.

- Composite Autonomic Symptom Score (COMPASS 31)

  The Composite Autonomic Symptom Score (COMPASS 31) (102) is a validated score that assesses the severity of symptoms and the autonomic functional capacity of patients with autonomic disorders. COMPASS 31 includes 31 selected questions of the well-established ASP (Autonomic Symptom Profile), a comprehensive 169 questions questionnaire assessing autonomic symptoms across multiple domains. COMPASS 31 is a refined, internally consistent, and

shortened quantitative measure of autonomic symptoms, which, thanks to a simplified scoring algorithm, is suitable for widespread use in autonomic research and practice. The 31 selected questions are divided into 6 main domains: orthostatic intolerance (i.e., dizziness after standing up), vasomotor (i.e., skin color changes), secretomotor (i.e., sweating, dry eyes), gastrointestinal (i.e., constipation, diarrhea), bladder dysfunctions (i.e., difficulty passing urine) and pupillomotor (i.e., photophobia). Each domain has a weighting factor based on its relevance, with factors adjusted so that the minimum total score is 0 and the maximum score is 100. Moreover, a new, more straightforward system for scoring autonomic symptoms was created. For example, simple yes/no questions resulted in a score of 1 point for yes and 0 points for no; questions about a particular symptom were given a score of 0 if it was not present and 1 if it was; all questions about the frequency of symptoms were given a score of 0 for rarely or never, 1 for occasionally, 2 for frequently, and 3 for almost always or constantly.

3.3 Optical coherence tomography

As explained in the previous chapter, OCT can produce cross-sectional images of biological systems at the micrometer scale. By directing a focused beam of light at the tissue to be imaged, then measuring the echo delay time for the light to be reflected from different microstructural features in the tissue, a cross-sectional image is constructed. OCT can attain spatial resolutions of 10 microns or less and does not require direct contact with the tissue being scanned (103). Even though it can be applied in many different medical fields, thanks to the transparency of the eye, OCT soon became a widely used ophthalmic diagnostic tool. The following retinal layers can be segmented and measured: ILM, RNFL, GCL, IPL, INL, OPL, ONL, ELM, PRC, RPE and Bruch’s membrane (BM) (104).

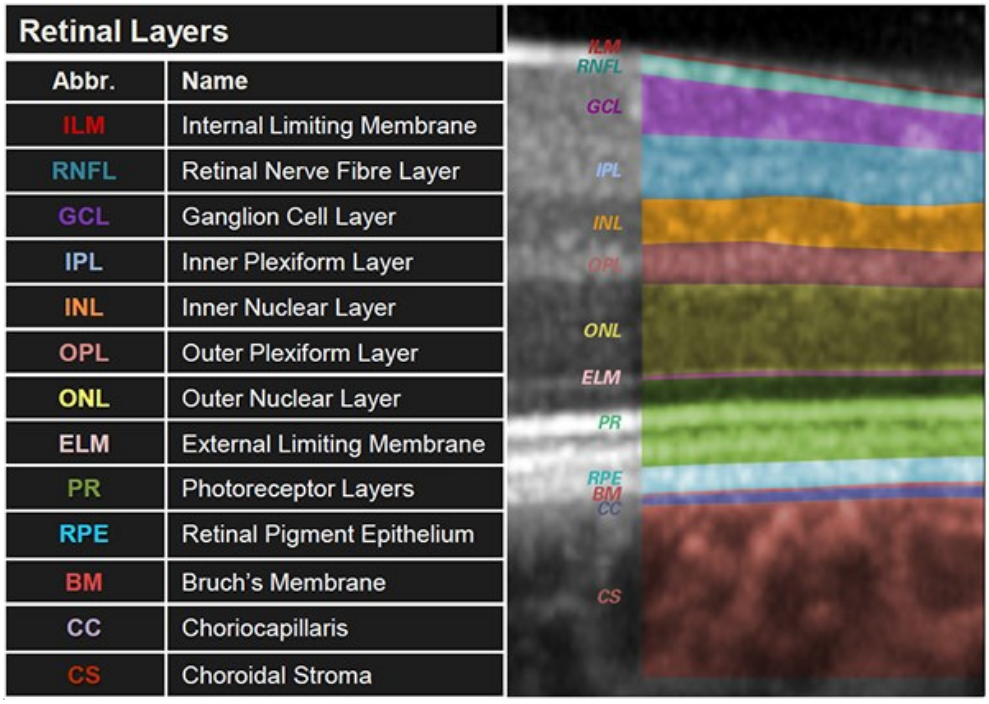

Fig. 8 – Retinal layers in Heidelberg's Spectralis OCT. Adapted from: Heidelberg Engineering "Retinal layers" Handout.

All subjects underwent optical coherence tomography imaging using SPECTRALIS® HRA+OCT (Heidelberg Engineering, Heidelberg, Germany), that combines SD-OCT technology with laser scanning confocal ophthalmoscopy (cSLO) with infrared wave (IR, 820 nm). TruTrack™ Active Eye Tracking, a patented technology that uses a second laser beam to actively track the eye during OCT scanning to avoid motion artifact, was used. The result is a punctual correlation between fundus oculi and OCT scans, associated with improvement of image definition and sharpness. Both eyes (OD and OS) were examined by experts, in a dim light and without the use of mydriatic agents.

The protocol included:

- 3.4 mm diameter circular peripapillary scan centred on the head of the optic nerve to measure the thickness of the RNFL (µm), expressed as both as global (pRNFL) and as individual temporal (T), temporal sectors superior (TS), inferior temporal (TI), papillomacular tract (PMB), nasal (N), superior nasal (NS), inferior nasal (NI). ART (Automatic Real-Time) system, which increases image quality by reducing motion artifacts and optimizing the signal-to-noise ratio, has

been used in each scan. Images with an ART between 90 and 100 were considered valid;

- 20x20° volumetric macular scan automatically centred on the fovea and obtained with 25 vertical B-scans (distance between B-scans 240 µm), ART 49. The software allows the evaluation of the macular volume total (VM), calculated as the volume subtended by a surface area defined by a circle having the fovea as its centre and a radius of 2 mm. The internationally recognized 9-segment ETDRS (Early Treatment Diabetic Retinopathy Screening) map subfield measurements were performed using the inbuilt Spectralis mapping software. Measurements are automatically averaged across each of the following subfields and sectors: the central fovea subfield within the inner 1-mm-diameter circle; the inner circle subfield between the inner and middle 3-mm-diameter circles; and the outer circle subfield between the middle and outer 6-mm-diameter circles. Both the inner and the outer circles were sectioned into superior, nasal, inferior, and temporal quadrants.

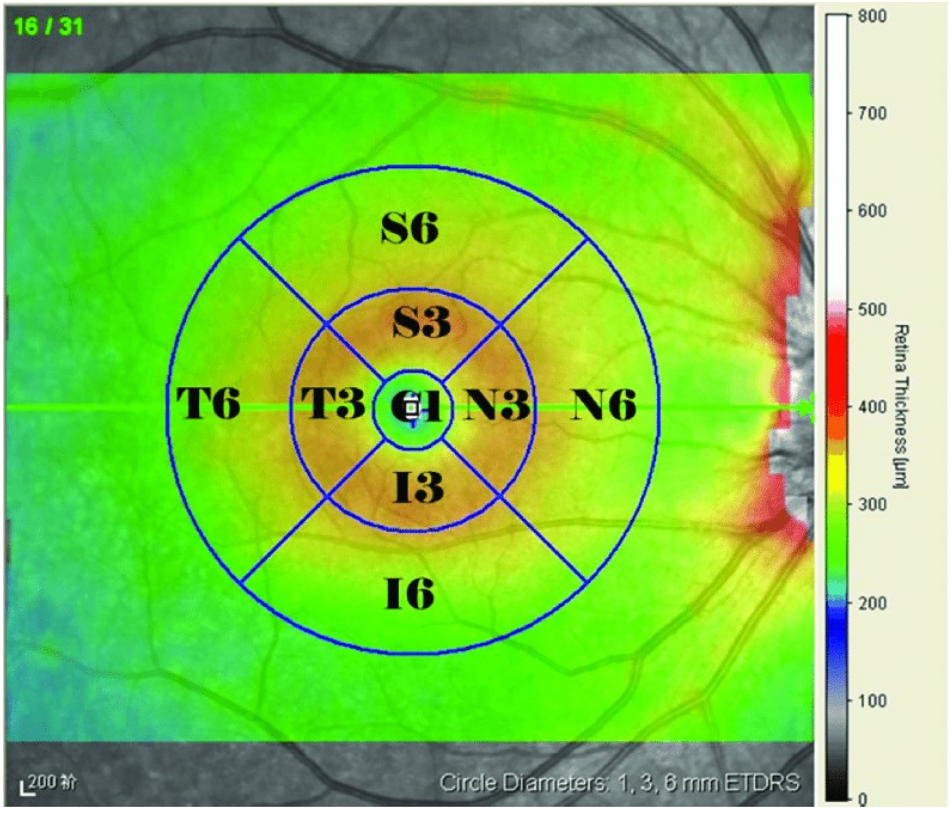

Fig. 9 - Representative Spectralis SD-OCT scans with macular thickness map (ETDRS grid). C1: the central fovea subfield/sector; S3, I3, T3, N3: superior,

inferior, temporal, and nasal sectors, respectively, of the inner circle subfield between 1and 3mm; S6, I6, T6, N6: superior, inferior, temporal, and nasal sectors, respectively, of the outer circle subfield between 3and 6mm. Adapted from: Li et al. (105)

For each macular scan, the Spectralis software automatically segmented the different retinal layers (RNFL, GCL, IPL, INL, OPL, ONL, RPE).

The following parameters of the macular scans were considered: total volume of retinal layers RNFL, GCL, IPL, INL, OPL, ONL, RPE, IRL (comprising the RNFL, GCL, IPL and INL layers) and ORL (outer retinal layers, comprising the OPL, ONL and RPE layers), total retinal volume, and total thickness of the retina and retinal layers.

The inner ring sectors (i.e., S1, I1, N1, T1) were grouped into a single data (IR) representing the average among the inner ring thicknesses, and the same was done with the outer ring sectors; the thickness values in S2, I2, N2, T2 were averaged to obtain the OR data. This was done to overcome the problem of specularity between nasal and temporal sectors between the two eyes.

Each SD-OCT scan was then re-evaluated by an experienced neurologist, in order to apply, if necessary, a manual correction of the segmentation, thus ensuring the accuracy of the stratification.

Low quality scans (<15 dB) according to OSCAR-IB criteria (106) were not included in the analysis: in particular, adequate scans of only one eye were obtained for 3 MSA patients, no scan could be acquired for 2 MSA patients, for 1 PD patient only the peripapillary and for 1 PD patient only the macular scans of one of the two eyes were acquired.

3.4 Hyperreflective retinal foci (HRF)

In line with recent publications (95,107), the analysis of the central linear scan of the macular map, crossing the fovea, was considered for HRF counting. HRF were identified as isolated punctiform elements of small dimensions (≤30μm) with intermediate reflectivity (similar to that of the RNFL) and without a shadow cone. HRF were counted in the central 3 mm, included

between two perpendicular lines to Bruch's Membrane traced at 1500 μm both temporally and nasally from the centre of the fovea. The count was performed in GCL, IPL and INL separately.

3.5 Skin biopsy

Two punch-biopsies of the skin (ø = 3mm; depth 3±2 mm) were performed at the cervical C7 paravertebral area after injecting lidocaine to ensure local anaesthesia. Sampled biopsies were collected in sterile Phosphate Buffered Solution (PBS) and subsequently underwent RT-QuIC (3.5.1) and histopathological evaluation via IHC (3.5.2).

3.5.1 RT-QuIC

Tissues were immediately frozen in N2 for further analyses by RT-QuIC. According to previously published procedures (74), tissue samples were first washed two times in ice cold PBS supplemented with protease inhibitor (PI) cocktail (Roche) to remove possible blood residues. Subsequently, skin samples were homogenized in PBS supplemented with PI cocktail at 1% w/v in gentleMACS™ M Tubes through gentleMACS™ Dissociator according to the manufacturer's protocol for protein extraction. Black 96-well plates with a clear bottom (Nalgene Nunc International) were pre-loaded with six 0.8 mm silica beads (OPS Diagnostics) per well. Tissue samples were thawed and vortexed 10s before use. Two μL of skin homogenates were added as seed to trigger the reaction in 98 μL of buffer containing 40 mM PB, pH 8.0, 170 mM NaCl, 10 μM thioflavin-T (ThT), and 0.1 mg/ml of recombinant α-Syn filtered using a 100 kDa MWCO filter (Millipore). The plate was sealed with a plate sealer film (Nalgene Nunc International) and incubated into Fluostar Omega (BMG Labtech) plate reader at 42 °C with intermittent double orbital shaking at 400 rpm for one minute, followed by 1-min rest. ThT fluorescence measurements were taken every 45 min using 450 nm excitation and 480 nm emission filter to overcome possible batch-to-batch variations of α-Syn

activity and intrinsic plate-to-plate experimental variability, relative fluorescent units (RFU) for every time point were normalized for the maximum intensity reached in each plate by the positive control and expressed in percentage.

Samples were run in quadruplicates and deemed positive when the replicate reached the threshold. The latter was calculated as the average normalized fluorescence value of negative control replicates during the first 10 hours of all runs, plus 30 standard deviations. The cut-off was differently set-up based on tissue sample at 45 hours for skin. When only one replicate crossed the threshold, the analysis was considered "unclear" and repeated up to three times.

A unified skin score of α-syn seeding activity was then calculated. The rate of positive replicates out of four replicates per sample was calculated, as was similarly described in previous studies (74,108–110). The rate of positive replicates was then averaged for each subject resulting in a specific score for each participant, further referred to as the “skin RT-QuIC score”, ranging from 0 to 1. A score of at least 0.5 was considered clearly positive, and a score of ≤0.25 was considered negative. An intermediate score between 0.25 and 0.5 was included.

All RT-QuIC experiments were performed at ISNB-Lab. of Prof. Parchi (UNIBO).

For α-Syn RT-QuIC data, statistical analysis and plot fluorescence values were performed using GraphPad Prism 9. The time required to reach the threshold (lag phase), were extracted for each sample replicate.

3.5.2 Histopathological evaluation

Biopsies were fixed for 24-48h at 4°C in Zamboni solution, paraffin-embedded and sectioned as 5µm thick sections at the rotary microtome (Leica RM2155). Haematoxylin and Eosin staining was employed for routine histopathological evaluation. Immunoperoxidase staining was performed on a Dako EnVision Autostainer (Dako Denmark A/S, Glostrup,

Denmark) according to manufacturer recommendations. Antibodies for phosphorylated alpha-synuclein Ser129 (Monoclonal Rabbit, dilution 1:1000, XXX), aggregated αSyn (Monoclonal Mouse, Clone 5G4, dilution 1:20.000, Millipore) and PGP9.5 (Polyclonal Rabbit, dilution 1:300, Abcam; Monoclonal Mouse, dilution 1:1000, Thermo-Fisher) were employed for single- and double-label immunoperoxidase staining, as well as immunofluorescent staining. Antigen retrieval was performed on a PT-Link Dako Antigen retrieval station using Citrate-buffer at pH 6 solution at 96° for 15 minutes, followed by 1 minute 95% formic acid for the αSyn-5G4 antibody. Slides were evaluated by an experienced pathologist and accordingly scored.

3.5.2.1 Immunoperoxidase staining

Immunoperoxidase staining was performed on a Dako EnVision Autostainer (Dako Denmark A/S, Glostrup, Denmark) according to manufacturer recommendations and in accordance to previously established protocols (111). Immunoperoxidase staining was repeated at least three times to ensure reaction consistency.

3.5.2.2 Immunofluorescence and confocal microscopy

Fluorescent immunohistochemistry was performed manually. Antigen retrieval was performed on de-paraffinized tissue as in immunoperoxidase staining methods. Following autofluorescence was quenched with a 50 mM NH4Cl solution for 10 minutes. Sections were treated with permeabilization and blocking solution (15% vol/vol Goat Serum, 2% wt/vol BSA, 0.25% wt/vol gelatin, 0.2% wt/vol glycine in PBS) containing 0.5% Triton X100 for 90 minutes before primary antibodies incubation. Primary antibodies were diluted in blocking solution and incubated at 4°C overnight. Alexa-Fluor plus 488 Goat anti-Mouse secondary antibody (A32723, Thermo Fisher Scientific) and Alexa-Fluor plus 568 anti-Rabbit secondary antibody (A-11011, Thermo Fisher Scientific) were diluted 1:200 in blocking solution as above and incubated for 60 minutes at room temperature. Hoechst 33258 were used for nuclear staining (Invitrogen, dilution: 1:10000 in PBS) for 10 minutes. Slides were mounted and coverslipped with Mowiol solution (Novabiochem)36. Confocal immunofluorescence z-stack images were

acquired on a Leica SP5 Laser Scanning Confocal Microscope using a HC PL FLUOTAR 20x/0.50 Dry or HCX PL APO lambda blue 40X/1.40 Oil objectives. Images were acquired at a 16-bit intensity resolution over 2048 × 2048 pixels. Z-stacks images were converted into digital maximum intensity z-projections, processed, and analyzed using ImageJ software.

3.6 Statistical analysis

The differences among the demographic variables present between the PD and MSA groups and healthy subjects were evaluated both for continuous and discrete variables by analysis of variance (ANOVA), performed by the Kruskal-Wallis nonparametric test, followed by the post-hoc Mann-Whitney test.

The differences present between the various groups for the OCT parameters were evaluated by analysis of variance (ANOVA) performed by the Kruskal-Wallis nonparametric test.

The possible linear correlation between OCT parameters and the demographic and clinical variables (age, disease duration, UMSARS and MDS-UPDRS) was then verified with multiple linear regression tests.

In the statistical analysis of the OCT data, it must be taken into consideration that two measurements are performed for each patient, one for each eye, and the intra-patient difference for the two eyes can also be non-negligible. For this reason, it is necessary to use a specific statistical model (GEE, Generalized Estimating Equation) which allows the analysis of repeated measures on the same subject, without a priori limits on the normal distribution of the variance within-subjects, allowing the inclusion in the model not only of possible errors between repeated measures but also of pathology-specific lateralization factors, as theorized by the recommendations for quantitative studies on OCT (APOSTEL criteria) (112).

The HRF data were evaluated by analysis of covariance (ANCOVA) performed by the Kruskal-Wallis nonparametric test, followed by post-hoc comparisons test.

The possible linear correlation between skin biopsy parameters and the clinical variables (age, disease duration, UMSARS and MDS-UPDRS, COMPASS31) was evaluated with the Spearman rank correlation coefficient and then verified with multiple linear regression tests.

The difference is considered statistically significant if the p-value is < 0.05.

4. Results

4.1 Clinical characteristics of the study population

During the study, 38 patients and 10 HC participants were recruited.

Twenty-four (24) patients (7 females, 17 males, mean age 63.5 ± 7.5) were diagnosed with PD according to the Movement Disorder Society PD Criteria (28), with a mean disease duration of 2.5 ± 1.4 years.

Fourteen (14) patients (9 females, 5 males, mean age 63.3 ± 10.5) were diagnosed with MSA according to the Second consensus statement on the diagnosis of multiple system atrophy criteria (54), with a mean disease duration of 4.2 ± 0.9 years. Seven (7) patients (4 females, 3 males, mean age 61.3 ± 11.7) showed cerebellar signs and was therefore classified as MSA-c, whereas seven (7) patients (5 females, 2 males, mean age 65.4 ± 9.6) showed parkinsonism and was classified as MSA-p.

Ten (10) healthy subjects (6 females, 4 males, mean age 51.3 ± 8.5) with no evidence of neurological or psychiatric disorders were included as controls.

All PD patients, 12 MSA patients and all HCs underwent OCT. 14 PD patients and 13 MSA patients underwent skin biopsy.

As shown in Table V, no significant differences in mean age and disease duration were found between the MSA and PD patient subgroups. The mean age of patients (MSA and PD) was higher than the mean age of healthy subjects (p-value = 0.002). The male percentage in the PD subgroup (70%) was found higher than in the MSA and HC subgroup (p-value=0.02). Disease duration was longer in MSA patients (p-value=0.001).

	HC N=10		MSA N=14		PD N=24		Kruscal Wallis ANOVA	Mann-Whitney post-hoc test		
	Mean	SD	Mean	SD	Mean	SD	P-value	HC vs. MSA	HC vs. PD	PD vs. MSA
Age	51,3	8,5641	63,3	10,488	63,583	7,5991	**0,0027**	x	X	
Sex (M%)	40%		36%		70%		**0,0235**			
Disease duration (years)			4,15	0,9466	2,526	1,4268	**0,0012**			

Table V – Demographic characteristics of the study population. SD=standard deviation.

4.2 Clinical evaluation

- MDS-Unified Parkinson's Disease Rating Scale (MDS-UPDRS)

  All PD patients were clinically evaluated with the MDS-Unified Parkinson's Disease Rating Scale (MDS-UPDRS). The mean global score was 20.8 ± 11.6. The mean scores in the different sections of the scale were as follows: MDS-UPDRS I 3.5 ± 3.6, MDS-UPDRS II 3.3 ± 2.9, MDS-UPDRS III 14.1 ± 8.7 (Table VI).

	Mean	SD
MDS-UPDRS I	3.458	3.635
MDS-UPDRS II	3.25	2.922
MDS-UPDRS III	14.125	8.749
MDS-UPDRS total score	20.833	11.593

Table VI – mean MDS-UPDRS scores in PD patients

- Unified Multiple System Atrophy Rating Scale (UMSARS)

  All MSA patients were clinically evaluated with the Unified Multiple System Atrophy Rating Scale (UMSARS). The mean global score was 36.3 ± 19.1/109. The mean scores in the different sections of the scale

were as follows: 15.9 ± 10 in UMSARS I, 18.3 ± 8.7 in UMSARS II and 2.2 ± 1.2 in UMSARS IV (Table VII).

	Mean	SD
UMSARS I	15.857	9.975
UMSARS II	18.285	8.695
UMSARS IV	2.214	1.188
UMSARS total score	36.357	19.052

Table VII – mean UMSARS scores in MSA patients

- Composite Autonomic Symptom Score (COMPASS 31)

  Both PD and MSA patients were additionally evaluated using the Composite Autonomic Symptom Score (COMPASS 31). Both the total COMPASS 31 score and the 6 domains [OH, vasomotor, secretomotor, gastrointestinal (GI), genitourinary (GU) and pupillomotor] scores were calculated.

  In PD patients, the mean scores in the different domains were as follows: OH 1.9 ± 6.6, vasomotor 0.4 ± 0.9, secretomotor 3.8 ± 4.2, GI 2.8 ± 3.1, GU 0.3 ± 0.8, pupillomotor 0.7 ± 1.1. The mean COMPASS 31 total score in PD patients was 9.8 ± 14.3.

  In MSA patients, the mean scores in the different domains were as follows: OH 10.3 ± 12, vasomotor 0, secretomotor 4.4 ± 2.6, GI 5.5 ± 2.2, GU 1.7 ± 1.6, pupillomotor 0.4 ± 1. The mean COMPASS 31 total score in MSA patients was 22.3 ± 15 (Table VIII).

  MSA patients showed higher scores in the GI (p-value=0.009) and GU (p-value=0.000) domains when compared to PD patients.

	PD		**MSA**		**Kruskal Wallis ANOVA**
	mean	SD	Mean	SD	p-value
Total OH	1.92	6.645	10.285	12.021	0.0623
Total Vasomotor	0.365	0.930	0	0	0.1670
Total Secretomotor	3.766	4.247	4.432	2.582	0.5877
Total GI	2.776	3.075	5.467	2.231	**0.0097**
Total GU	0.310	0.752	1.665	1.554	**0.0004**
Total Pupillomotor	0.673	1.100	0.447	1.064	0.1097

COMPASS31 Total score	9.812	14.346	22.298	14.952	0.377

Table VIII – Mean total and domain COMPASS 31 scores in PD and MSA patients

4.3 Optical coherence tomography

Table IX shows the mean values for pRNFL thickness in μm of the study population. The following data were considered:

- mean global thickness (G);
- mean thickness of the papillomacular bundle (PMB);
- ratio between the nasal and temporal fields (N/T ratio);
- mean thickness of the nasal (N), nasal inferior (NI) and nasal superior (NS) fields;
- mean thickness of the temporal (T), temporal inferior (TI) and temporal superior (TS) fields;

	HC N=10		MSA N=9		PD N=23		Kruskal Wallis Anova
	Mean	SD	Mean	SD	Mean	SD	P value
RNFLMean_G	97,2	8,4433	100,333	12,0986	98,696	11,4938	0,649082
RNFLMean_PMB	51,9	4,9148	55	8,2651	52,609	7,3762	0,733435
RNFL_NT_Ratio	1,115	0,1771	1,175	0,3811	1,152	0,24	0,895469
RNFLMean_NS	107,65	8,4428	111,5	21,5203	109,63	15,9838	0,529859
RNFLMean_N	73,1	11,462	77,944	16,6929	75,065	10,7833	0,922848
RNFLMean_NI	115,9	17,7948	126,111	25,4236	120,13	16,3264	0,498947
RNFLMean_TI	142,05	14,9247	138,278	34,241	140,457	25,5645	0,961048
RNFLMean_T	65,9	4,9933	68,722	10,106	67,152	10,8433	0,856551
RNFLMean_TS	134,05	13,502	132,944	14,5332	135,065	22,3094	0,911243

Table IX – mean peripapillary thickness in μm of the pRNFL

No statistically significant differences were found.

The following data were obtained from the macular scans:

- total volume (TV) in mm^3 of the different retinal layers and of the retina as a whole;
- mean thickness in μm of the different retinal layers divided in inner ring (IR) and outer ring (OR);

Data from the macular scans are shown in table X.

	HC N=10		MSA N=9		PD N=23		Kruskal Wallis Anova
	Mean	SD	Mean	SD	Mean	SD	P value
NFL mean IR	20,663	1,0342	18,819	7,3413	21,717	3,0454	**0,027165**
NFL mean OR	32,775	3,1846	30,153	11,6898	35,641	6,3784	0,054313
NFL_TotalVolume__mm³_	0,833	0,06734	0,764	0,2953	0,903	0,1544	**0,03238**
GCL mean IR	50,463	4,6398	44,347	17,4966	49,924	7,4177	0,704745
GCL mean OR	35,425	3,0891	31,403	12,4596	34,304	4,5982	0,932781
GCL_TotalVolume__mm³_	1,078	0,08997	0,953	0,3763	1,054	0,142	0,959488
IPL mean IR	41,016	3,4958	36,597	14,2331	40,761	5,3817	0,787945
IPL mean OR	28,913	2,2608	26,083	10,1741	28,223	3,5917	0,977694
IPLTotalVolume__mm³_	0,889	0,06464	0,796	0,3093	0,872	0,1104	0,993446
INL mean IR	38,138	3,0965	33,556	13,0039	38,098	4,2785	0,390642
INL mean OR	32,638	1,9107	28,014	10,5847	31,201	3,7386	0,199612
INL_TotalVolume__mm³_	0,945	0,05104	0,817	0,3092	0,917	0,1052	0,303218
OPL mean IR	32,45	2,8039	29,167	11,2604	32,804	5,1702	0,784551
OPL mean OR	27,712	2,037	23,958	9,0251	27,261	3,0165	0,291595
OPL_TotalVolume__mm³_	0,81	0,05968	0,707	0,2666	0,805	0,0958	0,993446
ONL mean IR	70,237	7,9413	63,125	24,7538	71,522	11,1447	0,63315
ONL mean OR	57,425	5,864	50,292	19,893	55,957	9,7147	0,886949
ONL_TotalVolume__mm³_	1,727	0,1802	1,532	0,6001	1,711	0,2813	0,948442
RPE mean IR	16	1,1667	14,042	5,3978	16,332	2,1074	0,085897
RPE mean OR	14,3	0,9321	12,778	4,9972	14,62	2,0448	0,232027
RPE_TotalVolume__mm³_	0,415	0,02369	0,372	0,145	0,427	0,05732	0,105681
IRL mean IR	253,475	12,9428	225,556	84,9742	254,777	29,0001	0,228379
IRL mean OR	214,85	10,6951	189,722	71,6955	212,658	25,993	0,457565
IRL_TotalVolume__mm³_	6,277	0,2914	5,566	2,0982	6,26	0,742	0,275509
ORL mean IR	82,487	2,3632	71,139	26,9055	81,005	8,8722	0,120542
ORL mean OR	78,987	2,284	68,792	25,9668	78,027	8,7108	0,051075
ORL_TotalVolume__mm³_	2,266	0,06235	1,967	0,7426	2,232	0,2468	**0,047739**
Retina mean IR	335,925	14,2044	296,708	111,7691	335,826	37,2872	0,202722
Retina mean OR	293,725	12,2126	258,611	97,6778	290,658	33,9321	0,262881
Retina_TotalVolume__mm³_	8,542	0,3388	7,533	2,8401	8,492	0,9717	0,126112

Table X – Mean thickness (µm) and volume (mm³) values in macular scans of the different retinal layers and of the retina as a whole

Mean thickness of the NFL in the IR section and total volume of both NFL and ORL in MSA patients were significantly lower than in PD patients and HCs. However, they did not survive the Bonferroni corrected threshold of $p<0.001$.

HRF were counted in the INL, in the GCIP (GCL + IPL) and in the IRL (INL + GCL + IPL). Table XI shows the data regarding HRF counting. It is evident that not only the number of HRF is higher in the patients' subgroup as opposed to HC, but PD patients present a higher number of HRF than MSA patients (p-value<0.001).

	PD		MSA		HC		ANCOVA
	mean	SD	mean	SD	mean	SD	p-value
HRF INL	22.133	6.266	16.142	5.534	12.45	4.071	**<0.001**
HRF GCIP	45.111	14.514	31.333	6.865	21.15	5.622	**<0.001**
HRF IRL	67.244	19.101	47.476	10.166	33.6	7.936	**<0.001**

Table XI – Number of HRF in the study population

Fig.10 shows box plots representing the number of HRF in the different subgroups in the INL, GCIP and IRL.

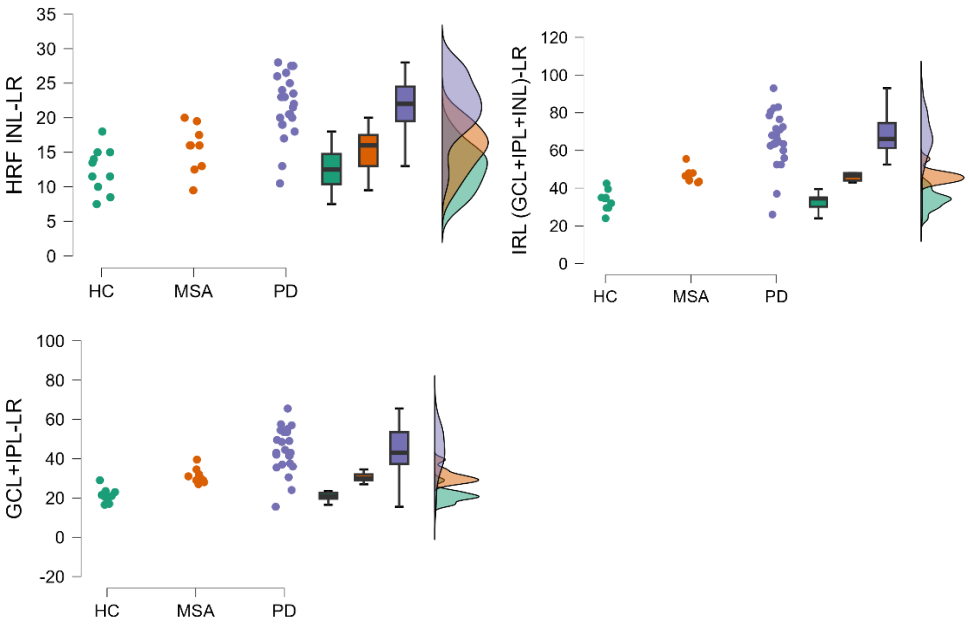

Fig.10 – Box plots representing the number of HRF in INL, GCIP and IRL in the study population

P-value between the MSA and the PD groups using Tukey's range test in post-hoc comparisons was found significant.

Fig.11 shows OCT cross-correlation patterns in HCs, PD and MSA patients.

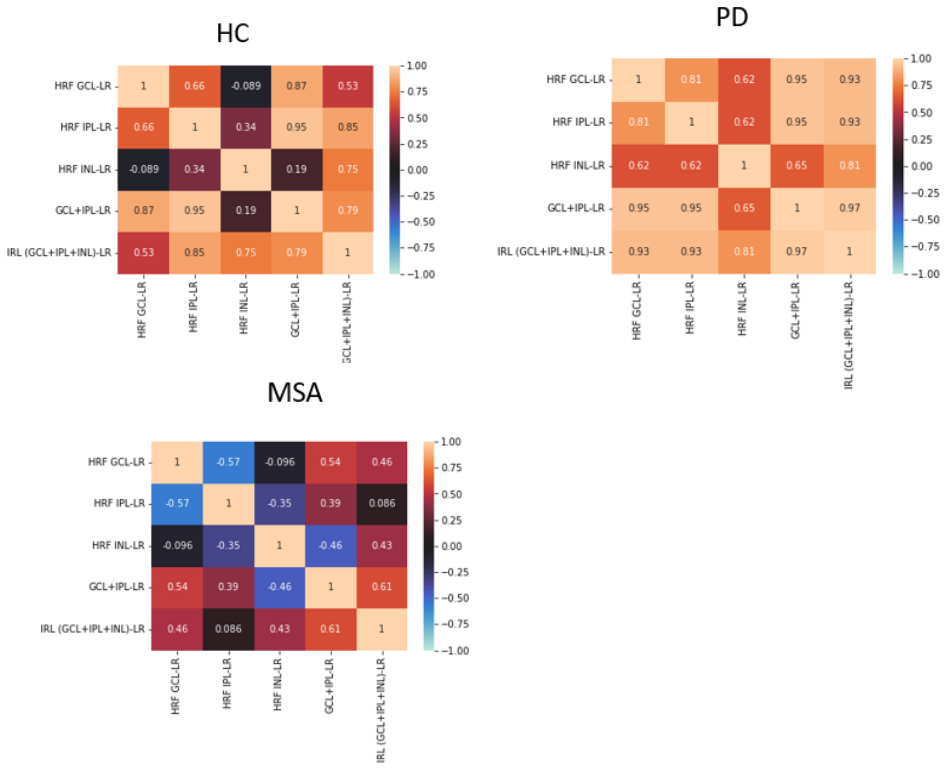

Fig.11 - OCT cross-correlation patterns in HCs, PD and MSA

No OCT measure reached significance after including in Least squares multiple regression vs. disease severity and COMPASS 31 scores.

4.4 Skin biopsy

Table XII shows the data regarding skin biopsies analyzed using RT-QuIC. RT-QuIC average score was 0.75 ± 0.9 in PD patients and 0.2 ± 0.5 in MSA patients.

Skin RT-QuIC score	**PD (total n.=12)**		**MSA (total n.=13)**	
Positive (≥0.5)	5		3	
Intermediate (>0.25; < 0.5)	0		0	
Negative (≤0.25)	7		10	
Average score (mean;SD)	0.75	0.920	0.2	0.483

Table XII – Skin RT-QuIC scores in PD and MSA patients

Table XIIIa-b shows the data regarding skin biopsies analyzed using IHC. Each biopsy was given a score ranging from 0 (no evidence of synucleinopathy) to 1. Scoring was based on four factors: phosphorylated alpha-synuclein deposition in vascular innervation (1), gland innervation (2), free nerve endings (3) and large dermal/hypodermal nerve fibers (4). Each factor was assigned a score of 0 (negative) and 1 (positive); the patient was considered positive for synucleinopathy if average score between the four factors was >0.25 (i.e., at least one factor had a score of 1). IHC average score was 0.32 ± 0.3 in PD patients and 0.27 ± 0.3 in MSA patients. Sensitivity was 71% and 67% in PD and MSA respectively.

IHC	**PD (total n.=14)**		**MSA (total n.=12)**	
0	4		4	
0.25	5		3	
0.50	3		4	
0.75	1		1	
1	1		0	
Average score (mean;SD)	0.321	0.301	0.275	0.275

Table XIIIa – Skin IHC average scores in PD and MSA patients

Anatomical localization of pSYN	**PD (total n.=14)**	**MSA (total n.=12)**
Vascular innervation	9	4
Glandular innervation	4	4
Free nerve endings	1	1
Hypodermal / dermal nerve bundles	4	5

Table XIIIb – Anatomical localization of pSYN immunoreactivity

No significant differences were found in either IHC or RT-QuIC average scores between the PD and MSA subgroups using the analysis of covariance (ANCOVA).

No statistically significant correlation was found between IHC and RT-QuIC scores in MSA patients.

As shown in tables XIV and XV, RT-QuIC scores correlate with UPDRS II, III and UPDRS total scores and with the OH and GU domain scores of the COMPASS 31 scale in PD patients. A linear correlation between these values was observed (Fig.12).

			UPDRS I Total	UPDRS II Total	UPDRS III Total	UPDRS Total score
PD	IHC AVERAGE	Correlation Coefficient	0,09	0,201	0,24	0,357
		Significance Level P	0,7594	0,4919	0,4077	0,2098
		n	14	14	14	14
	RT-QuIC	Correlation Coefficient	0,007	0,846	0,677	0,79
		Significance Level P	0,9855	**0,0021**	**0,0314**	**0,0066**
		n	10	10	10	10
	Spearman rank correlation coefficient					

Table XIV – Spearman rank correlation between IHC and RT-QuIC scores and UPDRS in PD patients.

			Total OH	Total Vasomotor	Total Secretomotor	Total GI	Total GU	Total Pupillomotor
PD	IHC AVERAGE	Correlation Coefficient	0,368	0,289	0,274	0,357	0,09	0,474
		Significance Level P	0,1948	0,3157	0,3426	0,2102	0,7602	0,0867
		n	14	14	14	14	14	14
	RT-QuIC	Correlation Coefficient	0,659	0,605	0,327	0,58	0,659	0,348
		Significance Level P	**0,0382**	0,0639	0,3567	0,0785	**0,0382**	0,3252
		n	10	10	10	10	10	10
	Spearman rank correlation coefficient							

Table XV – Spearman rank correlation between IHC and RT-QuIC scores and COMPASS 31 domains in PD patients.

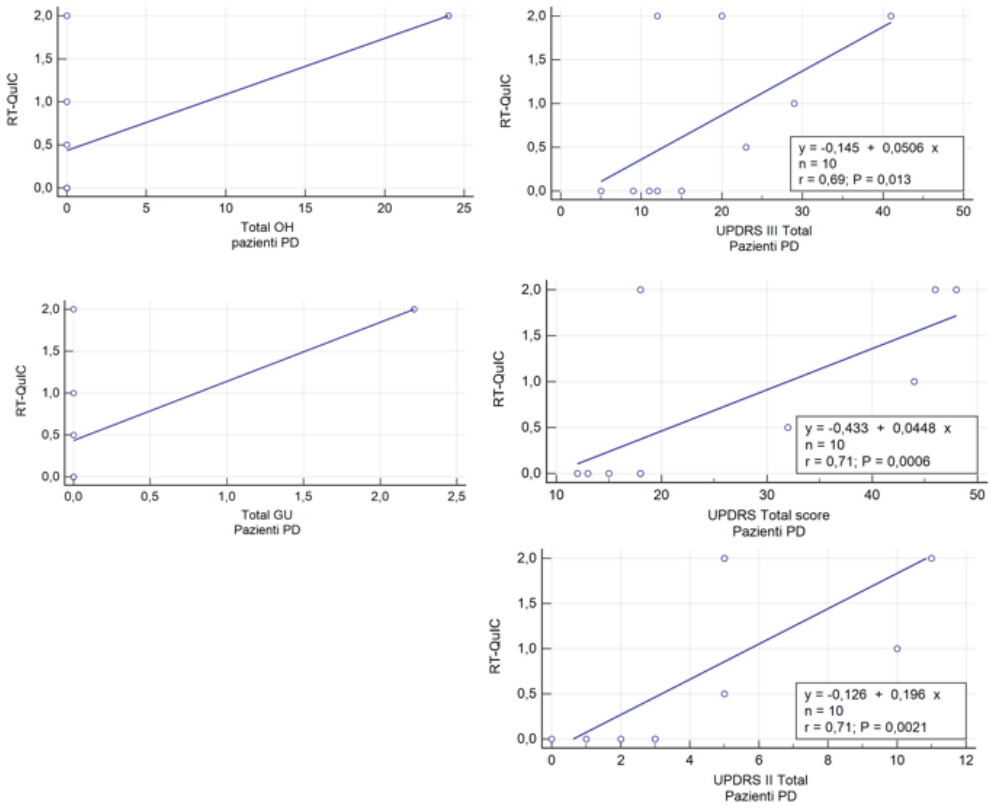

Fig.12 – Linear correlation between RT-QuIC scores and OH and GU domain scores (on the left) and UPDRS scores (on the right)

5. Discussion

The aim of this study is to define the role of OCT and skin biopsy in the early diagnosis and follow-up of PD and MSA and to assess them as possible tools in the differential diagnosis of α-synucleinopathies by identifying specific patterns.

OCT, a non-invasive exam providing high resolution images of the retina, has become an appealing candidate for the early diagnosis, follow-up and prognosis of neurodegenerative diseases. A meta-analysis by Chrysou et al. (83) shows that PD patients have significantly thinner retinas compared to age- and gender-matched controls. The pRNFL is affected mainly in the inferior, superior, and temporal regions, with an apparent sparing of the nasal sector. However, several studies (113–115) did not show any significant difference between PD patients and HCs. These findings are in line with our study, where no statistically significant difference was found between PD patients and HCs. Additionally, a meta-analysis by Zhou et al. (82), demonstrated a significant thinning in the macular region of the IRL and mGCC of PD patients and a strong association between PD and decreased macular thickness and volume. In this study, however, no correlation between OCT measures and MDS-UPDRS or COMPASS 31 scores was found.

The retinal damage in patients with MSA appears to follow a different pattern when compared with PD. A meta-analysis by Mendoza-Santiesteban et al. (90) found that, while in PD patients the atrophy of temporal pRNFL sectors and macular IRL (i.e., GCC) at the parafoveal region are prominent, in patients with MSA the inferior, superior and nasal pRNFL sectors are more affected than in PD. Several studies (116–118), however, did not report a significant difference. Our study is in line with these findings, showing no statistically significant correlation with either pRNFL or GCC. We did, however, find a significant thinning of the macular RNFL (part of the GCC) and of the ORL.

Global macular retinal thinning was observed in MSA, with a strong correlation with the patients' UMSARS scores (90). In this study, however,

no correlation between OCT measures and UMSARS scores or COMPASS 31 scores was found.

In our study, we also calculated the HRF number in the macular region. HRF are hyperreflective spots, whose aetiology remains unclear; however, one of the most accredited hypotheses suggests that HRF are essentially clusters of activated and proliferating microglia (119). Retinal microglia has the same morphological and functional features as CNS microglia: they are activated by damage-induced inflammatory reactions and are capable of releasing cytokines and activating the complement cascade (120). Even though to date no studies have been published about HRF counting in parkinsonisms, interest grew recently about its role as a possible biomarker in MS (95). Our results showed that the HRF number is higher in every layer considered (INL, GCIP, IRL) in the pathological subgroups (PD and MSA) when compared to the HCs. Moreover, the HRF count was higher in PD patients than in MSA patients. This could be linked to a greater retinal damage with subsequent microglial activation in PD patients or they might represent α-syn aggregates. However, more research is needed in order to validate these findings and to further investigate their aetiology.

The novel RT-QuIC seeding assay showed high sensitivity and specificity both in PD (with a diagnostic accuracy of 88.9%) (74) and in MSA (121). In previous studies (74), higher α-syn seeding activity in RT-QuIC also correlated with longer disease duration, more advanced disease stage and with the presence of RBD, cognitive impairment, and constipation. In our study, a statistically significant correlation was found between RT-QuIC scores and disease severity (UPDRS part II, III and UPDRS total score) and the OH and GU domains of the validated COMPASS 31 scale.

A meta-analysis by Tsukita et al. (70) demonstrated that the degree of α-syn deposition detected through IHC in cutaneous autonomic fibers increases in patients with PD. Sensitivity and specificity (respectively 76% and 100%) were higher in the skin when compared to gastrointestinal and submandibular gland samples. Other studies (122,123) also reported that skin biopsy sensitivity varies depending on the location of the sampling site with the posterior region of the neck showing the best sensitivity. This study, in line

with the meta-analysis' results, showed a paravertebral IHC skin biopsy sensitivity of 71% in PD patients. 4 PD patients showed no α-syn deposition in cutaneous autonomic fibers; this finding would support the theory that PD patients can be divided in a CNS-first and a PNS-first subtype (20). Furthermore, patients with specific genetic risk factors associated to PD (i.e., LRKK2, Parkin) do not consistently present α-syn pathology, both in the brain and the periphery. Sensitivity in MSA patients reached 67%, once again in line with the limited results from literature on the subject (124). A study by Wang et al. (125) found a correlation between IHC detection of α-syn in cutaneous autonomic fibers and disease stage (H&Y) and severity of autonomic symptoms of 20 PD patients (mean duration of disease 4.2 ± 3.7 years). In our study, we found no significant correlation; however, this could be due to the shorter disease duration of our subjects (2.5 ± 1.4 years).

The small sample size is the main limitation of this study. This is due to the fact that MSA is a rare disease with an annual incidence of only 0.6 per 100 000 and a prevalence of 1 to 4 in 100 000 (47). Another limitation is the lack of autopsy-confirmed diagnosis. Nevertheless, we selected only patients who fulfilled the validated clinical criteria, and the clinical diagnosis was supported by specific diagnostic tests. Additionally, OCT scan success was partly dependent on the patient's clinical state. Despite the presence of the algorithm to reduce motion artifacts, patient compliance and even saccadic movement can introduce image artifacts. Further enhancement and refinement of the processing algorithms will be needed to reduce these artifacts and improve the reliability.

6. Conclusions

Our study showed no significant differences regarding OCT parameters in patients with α-synucleinopathies.

However, this study indicates that HRF (found in significantly greater quantities in all pathological subgroups) are non-specific biomarkers of many neuropathological conditions; not only MS, but also PD and MSA. Further studies will be needed in order to validate the role of HRF counting in the early and differential diagnosis of α-synucleinopathies.

Our study also suggests that the detection of α-syn in skin biopsies -a minimally invasive, reliable and reproducible procedure- may be a useful tool in the early diagnosis of PD and MSA, but may also serve as a biomarker of disease progression in PD patients.

The present work is configured as a pilot study, underlining the need to continue investigating the use of OCT and skin biopsy in neurodegenerative diseases, possibly through a longitudinal study design with a larger sample size. Research should also focus on finding methods to further increase sensitivity and specificity of both OCT and skin biopsy in the early diagnosis of α-synucleinopathies in order to enable their use in standard clinical practice.

7. Bibliography

1. McCann H, Stevens CH, Cartwright H, Halliday G. α-SYNUCLEINOPATHY PHENOTYPES. Parkinsonism Relat Disord. 2014;20(Suppl. 1).

2. George JM. The synucleins. Genome Biol. 2002;3(1).

3. Calabresi P, Mechelli A, Natale G, Volpicelli-Daley L, Di Lazzaro G, Ghiglieri V. Alpha-synuclein in Parkinson's disease and other synucleinopathies: from overt neurodegeneration back to early synaptic dysfunction. Cell Death Dis. 2023 Mar 1;14(3):1–16.

4. Ltic S, Perovic M, Mladenovic A, Raicevic N, Ruzdijic S, Rakic L, et al. Alpha-synuclein is expressed in different tissues during human fetal development. J Mol Neurosci MN. 2004;22(3):199–204.

5. Bridi JC, Hirth F. Mechanisms of α-Synuclein Induced Synaptopathy in Parkinson's Disease. Front Neurosci. 2018;12.

6. Burré J. The Synaptic Function of α-Synuclein. J Park Dis. 2015 Jan 1;5(4):699–713.

7. Barba L, Paolini Paoletti F, Bellomo G, Gaetani L, Halbgebauer S, Oeckl P, et al. Alpha and Beta Synucleins: From Pathophysiology to Clinical Application as Biomarkers. Mov Disord. 2022;37(4):669–83.

8. Kim C, Lee SJ. Controlling the mass action of α-synuclein in Parkinson's disease. J Neurochem. 2008;107(2):303–16.

9. Tenreiro S, Eckermann K, Outeiro TF. Protein phosphorylation in neurodegeneration: friend or foe? Front Mol Neurosci. 2014;7.

10. Chu Y, Kordower JH. Age-associated increases of alpha-synuclein in monkeys and humans are associated with nigrostriatal dopamine depletion: Is this the target for Parkinson's disease? Neurobiol Dis. 2007 Jan;25(1):134–49.

11. Xilouri M, Brekk OR, Stefanis L. α-Synuclein and protein degradation systems: a reciprocal relationship. Mol Neurobiol. 2013 Apr;47(2):537–51.

12. Frost B, Diamond MI. Prion-like Mechanisms in Neurodegenerative Diseases. Nat Rev Neurosci. 2010 Mar;11(3):155–9.

13. Dorsey ER, Elbaz A, Nichols E, Abbasi N, Abd-Allah F, Abdelalim A, et al. Global, regional, and national burden of Parkinson's disease, 1990–2016: a systematic analysis for the Global Burden of Disease Study 2016. Lancet Neurol. 2018 Nov 1;17(11):939–53.

14. Poewe W, Seppi K, Tanner CM, Halliday GM, Brundin P, Volkmann J, et al. Parkinson disease. Nat Rev Dis Primer. 2017 Mar 23;3(1):1–21.

15. Armstrong MJ, Okun MS. Diagnosis and Treatment of Parkinson Disease: A Review. JAMA. 2020 Feb 11;323(6):548–60.

16. Global, regional, and national burden of Parkinson's disease, 1990–2016: a systematic analysis for the Global Burden of Disease Study 2016. Lancet Neurol. 2018 Nov;17(11):939–53.

17. Klein C, Westenberger A. Genetics of Parkinson's Disease. Cold Spring Harb Perspect Med. 2012 Jan;2(1).

18. Hilton DA, Shivane AG. Neurodegenerative Disorders. In: Hilton DA, Shivane AG, editors. Neuropathology Simplified: A Guide for Clinicians and Neuroscientists. Cham: Springer International Publishing; 2021. p. 159–76.

19. Braak H, Del Tredici K, Rüb U, de Vos RAI, Jansen Steur ENH, Braak E. Staging of brain pathology related to sporadic Parkinson's disease. Neurobiol Aging. 2003;24(2):197–211.

20. Borghammer P, Van Den Berge N. Brain-First versus Gut-First Parkinson's Disease: A Hypothesis. J Park Dis. 9(Suppl 2):S281–95.

21. Loscalzo, Joseph, Fauci, Anthony S., Kasper, Dennis L., Hauser, Stephen, Longo, Dan Louis, Jameson, J. Larry. Harrison's Principles of Internal Medicine. 21st ed. New York : McGraw Hill; 2022.

22. Jankovic J. Parkinson's disease: clinical features and diagnosis. J Neurol Neurosurg Psychiatry. 2008 Apr 1;79(4):368–76.

23. Rodriguez-Oroz MC, Jahanshahi M, Krack P, Litvan I, Macias R, Bezard E, et al. Initial clinical manifestations of Parkinson's disease: features and pathophysiological mechanisms. Lancet Neurol. 2009 Dec;8(12):1128–39.

24. Massano J, Bhatia KP. Clinical Approach to Parkinson's Disease: Features, Diagnosis, and Principles of Management. Cold Spring Harb Perspect Med. 2012 Jun;2(6).

25. Schapira AHV, Chaudhuri KR, Jenner P. Non-motor features of Parkinson disease. Nat Rev Neurosci. 2017 Jul;18(7):435–50.

26. Bloem BR, Okun MS, Klein C. Parkinson's disease. The Lancet. 2021 Jun 12;397(10291):2284–303.

27. Galbiati A, Verga L, Giora E, Zucconi M, Ferini-Strambi L. The risk of neurodegeneration in REM sleep behavior disorder: A systematic review and meta-analysis of longitudinal studies. Sleep Med Rev. 2019 Feb 1;43:37–46.

28. Postuma RB, Berg D, Stern M, Poewe W, Olanow CW, Oertel W, et al. MDS clinical diagnostic criteria for Parkinson's disease. Mov Disord. 2015;30(12):1591–601.

29. Tolosa E, Garrido A, Scholz SW, Poewe W. Challenges in the diagnosis of Parkinson's disease. Lancet Neurol. 2021 May;20(5):385–97.

30. Fereshtehnejad SM, Zeighami Y, Dagher A, Postuma RB. Clinical criteria for subtyping Parkinson's disease: biomarkers and longitudinal progression. Brain. 2017 Jul 1;140(7):1959–76.

31. Thanvi B, Lo N, Robinson T. Vascular parkinsonism—an important cause of parkinsonism in older people. Age Ageing. 2005 Mar 1;34(2):114–9.

32. Greenland JC, Barker RA. The Differential Diagnosis of Parkinson's Disease. In: Stoker TB, Greenland JC, editors. Parkinson's Disease: Pathogenesis and Clinical Aspects. Brisbane (AU): Codon Publications; 2018.

33. Massano J, Costa F, Nadais G. Teaching NeuroImage: MRI in multiple system atrophy: "Hot cross bun" sign and hyperintense rim bordering the putamina. Neurology. 2008 Oct 7;71(15):e38–e38.

34. Hoglinger GU, Respondek G, Stamelou M, Kurz C, Josephs KA, Lang AE, et al. Clinical Diagnosis of Progressive Supranuclear Palsy: The Movement Disorder Society Criteria. Mov Disord Off J Mov Disord Soc. 2017 Jun;32(6):853–64.

35. Shin HW, Chung SJ. Drug-Induced Parkinsonism. J Clin Neurol. 2012 Mar 1;8(1):15–21.

36. de Lau LML, Schipper CMA, Hofman A, Koudstaal PJ, Breteler MMB. Prognosis of Parkinson disease: risk of dementia and mortality: the Rotterdam Study. Arch Neurol. 2005 Aug;62(8):1265–9.

37. Poewe W, Mahlknecht P. The clinical progression of Parkinson's disease. Parkinsonism Relat Disord. 2009 Dec 1;15:S28–32.

38. Ropper, Allan H., Samuels, Martin A., Prasad, Sashank, Klein, Joshua. Adams and Victor's Principles of Neurology. 11th ed. New York : McGraw Hill; 2019.

39. John Van Geest Centre for Brain Repair, Department of Clinical Neurosciences, University of Cambridge, UK, Stoker TB, Greenland JC, John Van Geest Centre for Brain Repair, Department of Clinical Neurosciences, University of Cambridge, UK, editors. Parkinson's Disease: Pathogenesis and Clinical Aspects. Codon Publications; 2018.

40. Rascol O, Fabbri M, Poewe W. Amantadine in the treatment of Parkinson's disease and other movement disorders. Lancet Neurol. 2021 Dec 1;20(12):1048–56.

41. Sprenger F, Poewe W. Management of Motor and Non-Motor Symptoms in Parkinson's Disease. CNS Drugs. 2013 Apr 1;27(4):259–72.

42. Herrington TM, Cheng JJ, Eskandar EN. Mechanisms of deep brain stimulation. J Neurophysiol. 2016 Jan 1;115(1):19–38.

43. Martinez-Ramirez D, Hu W, Bona AR, Okun MS, Shukla AW. Update on deep brain stimulation in Parkinson's disease. Transl Neurodegener. 2015 Jun 27;4(1):12.

44. Deuschl G, Antonini A, Costa J, Śmiłowska K, Berg D, Corvol JC, et al. European Academy of Neurology/Movement Disorder Society - European Section guideline on the treatment of Parkinson's disease: I. Invasive therapies. Eur J Neurol. 2022;29(9):2580–95.

45. Saba RA, Maia DP, Cardoso FEC, Borges V, F. Andrade LA, Ferraz HB, et al. Guidelines for Parkinson's disease treatment: consensus from the Movement Disorders Scientific Department of the Brazilian Academy of Neurology -motor symptoms. Arq Neuropsiquiatr. 80(3):316–29.

46. Krismer F, Wenning GK. Multiple system atrophy: insights into a rare and debilitating movement disorder. Nat Rev Neurol. 2017 Apr;13(4):232–43.

47. Stefanova N, Bücke P, Duerr S, Wenning GK. Multiple system atrophy: an update. Lancet Neurol. 2009 Dec;8(12):1172–8.

48. Vanacore N. Epidemiological evidence on multiple system atrophy. J Neural Transm Vienna Austria 1996. 2005 Dec;112(12):1605–12.

49. Jellinger KA, Lantos PL. Papp-Lantos inclusions and the pathogenesis of multiple system atrophy: an update. Acta Neuropathol (Berl). 2010 Jun;119(6):657–67.

50. Fanciulli A, Wenning GK. Multiple-System Atrophy. N Engl J Med. 2015 Jan 15;372(3):249–63.

51. Wenning GK, Tison F, Seppi K, Sampaio C, Diem A, Yekhlef F, et al. Development and validation of the Unified Multiple System Atrophy Rating Scale (UMSARS). Mov Disord. 2004;19(12):1391–402.

52. Köllensperger M, Geser F, Ndayisaba JP, Boesch S, Seppi K, Ostergaard K, et al. Presentation, diagnosis, and management of multiple system atrophy in Europe: Final analysis of the European multiple system atrophy registry. Mov Disord. 2010;25(15):2604–12.

53. Palma JA, Norcliffe-Kaufmann L, Kaufmann H. Diagnosis of multiple system atrophy. Auton Neurosci. 2018 May 1;211:15–25.

54. Gilman S, Wenning GK, Low PA, Brooks DJ, Mathias CJ, Trojanowski JQ, et al. Second consensus statement on the diagnosis of multiple system atrophy. Neurology. 2008 Aug 26;71(9):670–6.

55. Koga S, Aoki N, Uitti RJ, Gerpen JA van, Cheshire WP, Josephs KA, et al. When DLB, PD, and PSP masquerade as MSA: An autopsy study of 134 patients. Neurology. 2015 Aug 4;85(5):404–12.

56. Quinn NP. How to diagnose multiple system atrophy. Mov Disord. 2005;20(S12):S5–10.

57. Meissner WG, Fernagut PO, Dehay B, Péran P, Traon APL, Foubert-Samier A, et al. Multiple System Atrophy: Recent Developments and Future Perspectives. Mov Disord. 2019;34(11):1629–42.

58. Perez-Lloret S, Flabeau O, Fernagut PO, Pavy-Le Traon A, Rey MV, Foubert-Samier A, et al. Current Concepts in the Treatment of Multiple System Atrophy. Mov Disord Clin Pract. 2015;2(1):6–16.

59. Riley DE. Orthostatic hypotension in multiple system atrophy. Curr Treat Options Neurol. 2000 May 1;2(3):225–30.

60. Singer W. Recent advances in establishing fluid biomarkers for the diagnosis and differentiation of alpha-synucleinopathies – a mini review. Clin Auton Res. 2022 Aug 1;32(4):291–7.

61. Magalhães P, Lashuel HA. Opportunities and challenges of alpha-synuclein as a potential biomarker for Parkinson's disease and other synucleinopathies. Npj Park Dis. 2022 Jul 22;8(1):1–26.

62. Paciotti S, Bellomo G, Gatticchi L, Parnetti L. Are We Ready for Detecting α-Synuclein Prone to Aggregation in Patients? The Case of "Protein-Misfolding Cyclic Amplification" and "Real-Time Quaking-Induced Conversion" as Diagnostic Tools. Front Neurol. 2018 Jun 6;9:415.

63. Nakagaki T, Nishida N, Satoh K. Development of α-Synuclein Real-Time Quaking-Induced Conversion as a Diagnostic Method for α-Synucleinopathies. Front Aging Neurosci. 2021 Sep 28;13:703984.

64. Parnetti L, Gaetani L, Eusebi P, Paciotti S, Hansson O, El-Agnaf O, et al. CSF and blood biomarkers for Parkinson's disease. Lancet Neurol. 2019 Jun 1;18(6):573–86.

65. Parnetti L, Farotti L, Eusebi P, Chiasserini D, De Carlo C, Giannandrea D, et al. Differential role of CSF alpha-synuclein species, tau, and Aβ42 in Parkinson's Disease. Front Aging Neurosci. 2014 Mar 31;6:53.

66. Oeckl P, Halbgebauer S, Anderl-Straub S, von Arnim CAF, Diehl-Schmid J, Froelich L, et al. Targeted Mass Spectrometry Suggests Beta-Synuclein as Synaptic Blood Marker in Alzheimer's Disease. J Proteome Res. 2020 Mar 6;19(3):1310–8.

67. Halbgebauer S, Oeckl P, Steinacker P, Yilmazer-Hanke D, Anderl-Straub S, Arnim C von, et al. Beta-synuclein in cerebrospinal fluid as an early diagnostic marker of Alzheimer's disease. J Neurol Neurosurg Psychiatry. 2021 Apr 1;92(4):349–56.

68. Oeckl P, Metzger F, Nagl M, von Arnim CAF, Halbgebauer S, Steinacker P, et al. Alpha-, Beta-, and Gamma-synuclein Quantification in Cerebrospinal Fluid by Multiple Reaction Monitoring Reveals Increased Concentrations in Alzheimer′s and Creutzfeldt-Jakob Disease but No Alteration in Synucleinopathies. Mol Cell Proteomics MCP. 2016 Oct;15(10):3126–38.

69. Doppler K, Ebert S, Üçeyler N, Trenkwalder C, Ebentheuer J, Volkmann J, et al. Cutaneous neuropathy in Parkinson's disease: a window into brain pathology. Acta Neuropathol (Berl). 2014 Jul 1;128(1):99–109.

70. Tsukita K, Sakamaki-Tsukita H, Tanaka K, Suenaga T, Takahashi R. Value of in vivo α-synuclein deposits in Parkinson's disease: A systematic review and meta-analysis. Mov Disord. 2019;34(10):1452–63.

71. Siepmann T, Penzlin AI, Illigens BMW, Reichmann H. Should Skin Biopsies Be Performed in Patients Suspected of Having Parkinson's Disease? Park Dis. 2017;2017:6064974.

72. Donadio V, Incensi A, Leta V, Giannoccaro MP, Scaglione C, Martinelli P, et al. Skin nerve α-synuclein deposits: a biomarker for idiopathic Parkinson disease. Neurology. 2014 Apr 15;82(15):1362–9.

73. Donadio V, Incensi A, Rizzo G, De Micco R, Tessitore A, Devigili G, et al. Skin Biopsy May Help to Distinguish Multiple System Atrophy–Parkinsonism from Parkinson's Disease With Orthostatic Hypotension. Mov Disord. 2020;35(9):1649–57.

74. Kuzkina A, Bargar C, Schmitt D, Rößle J, Wang W, Schubert AL, et al. Diagnostic value of skin RT-QuIC in Parkinson's disease: a two-laboratory study. Npj Park Dis. 2021 Dec 1;7.

75. Fujimoto JG, Pitris C, Boppart SA, Brezinski ME. Optical Coherence Tomography: An Emerging Technology for Biomedical Imaging and Optical Biopsy. Neoplasia N Y N. 2000 Jan;2(1–2):9–25.

76. Kolb H. Simple Anatomy of the Retina. In: Kolb H, Fernandez E, Nelson R, editors. Webvision: The Organization of the Retina and Visual System. Salt Lake City (UT): University of Utah Health Sciences Center; 1995.

77. Grzybowski A, Barboni P, editors. OCT and Imaging in Central Nervous System Diseases: The Eye as a Window to the Brain. 2nd ed. Cham: Springer International Publishing; 2020.

78. London A, Benhar I, Schwartz M. The retina as a window to the brain—from eye research to CNS disorders. Nat Rev Neurol. 2013 Jan;9(1):44–53.

79. Akopian A, Witkovsky P. D2 dopamine receptor-mediated inhibition of a hyperpolarization-activated current in rod photoreceptors. J Neurophysiol. 1996 Sep;76(3):1828–35.

80. Chaudhuri KR, Sauerbier A. Parkinson disease. Unravelling the nonmotor mysteries of Parkinson disease. Nat Rev Neurol. 2016 Jan;12(1):10–1.

81. Djamgoz MBA, Hankins MW, Hirano J, Archer SN. Neurobiology of retinal dopamine in relation to degenerative states of the tissue. Vision Res. 1997 Dec 1;37(24):3509–29.

82. Zhou WC, Tao JX, Li J. Optical coherence tomography measurements as potential imaging biomarkers for Parkinson's disease: A systematic review and meta-analysis. Eur J Neurol. 2021;28(3):763–74.

83. Chrysou A, Jansonius NM, van Laar T. Retinal layers in Parkinson's disease: A meta-analysis of spectral-domain optical coherence tomography studies. Parkinsonism Relat Disord. 2019 Jul 1;64:40–9.

84. Satue M, Obis J, Rodrigo MJ, Otin S, Fuertes MI, Vilades E, et al. Optical Coherence Tomography as a Biomarker for Diagnosis, Progression, and Prognosis of Neurodegenerative Diseases. J Ophthalmol. 2016;2016:8503859.

85. Lee JY, Martin-Bastida A, Murueta-Goyena A, Gabilondo I, Cuenca N, Piccini P, et al. Multimodal brain and retinal imaging of dopaminergic degeneration in Parkinson disease. Nat Rev Neurol. 2022 Apr;18(4):203–20.

86. Kwapong WR, Ye H, Peng C, Zhuang X, Wang J, Shen M, et al. Retinal Microvascular Impairment in the Early Stages of Parkinson's Disease. Invest Ophthalmol Vis Sci. 2018 Aug 10;59(10):4115–22.

87. Zhang J ru, Cao Y lan, Li K, Wang F, Wang Y li, Wu J jing, et al. Correlations between retinal nerve fiber layer thickness and cognitive progression in Parkinson's disease: A longitudinal study. Parkinsonism Relat Disord. 2021 Jan 1;82:92–7.

88. Mendoza-Santiesteban CE, Palma JA, Martinez J, Norcliffe-Kaufmann L, Hedges TR, Kaufmann H. Progressive Retinal Structure Abnormalities in Multiple System Atrophy. Mov Disord Off J Mov Disord Soc. 2015 Dec;30(14):1944–53.

89. Ahn J, Lee JY, Kim TW. Retinal thinning correlates with clinical severity in multiple system atrophy. J Neurol. 2016 Oct;263(10):2039–47.

90. Mendoza-Santiesteban CE, Gabilondo I, Palma JA, Norcliffe-Kaufmann L, Kaufmann H. The Retina in Multiple System Atrophy: Systematic Review and Meta-Analysis. Front Neurol. 2017;8.

91. Pilotto E, Miante S, Torresin T, Puthenparampil M, Frizziero L, Federle L, et al. Hyperreflective Foci in the Retina of Active Relapse-Onset Multiple Sclerosis. Ophthalmology. 2020 Dec 1;127(12):1774–6.

92. Bolz M, Schmidt-Erfurth U, Deak G, Mylonas G, Kriechbaum K, Scholda C. Optical Coherence Tomographic Hyperreflective Foci: A Morphologic Sign of Lipid Extravasation in Diabetic Macular Edema. Ophthalmology. 2009 May 1;116(5):914–20.

93. Framme C, Wolf S, Wolf-Schnurrbusch U. Small Dense Particles in the Retina Observable by Spectral-Domain Optical Coherence Tomography in Age-Related Macular Degeneration. Invest Ophthalmol Vis Sci. 2010 Nov 1;51(11):5965–9.

94. Uji A, Murakami T, Nishijima K, Akagi T, Horii T, Arakawa N, et al. Association Between Hyperreflective Foci in the Outer Retina, Status of Photoreceptor Layer, and Visual Acuity in Diabetic Macular Edema. Am J Ophthalmol. 2012 Apr 1;153(4):710-717.e1.

95. Pengo M, Miante S, Franciotta S, Ponzano M, Torresin T, Bovis F, et al. Retinal Hyperreflecting Foci Associate With Cortical Pathology in Multiple Sclerosis. Neurol Neuroimmunol Neuroinflammation. 2022 May 23;9(4):e1180.

96. Colonna M, Butovsky O. Microglia Function in the Central Nervous System During Health and Neurodegeneration. Annu Rev Immunol. 2017 Apr 26;35:441–68.

97. Garcia P, Jürgens-Wemheuer W, Uriarte Huarte O, Michelucci A, Masuch A, Brioschi S, et al. Neurodegeneration and neuroinflammation are linked, but independent of alpha-synuclein inclusions, in a seeding/spreading mouse model of Parkinson's disease. Glia. 2022;70(5):935–60.

98. Vieira BDM, Radford RA, Chung RS, Guillemin GJ, Pountney DL. Neuroinflammation in Multiple System Atrophy: Response to and Cause of α-Synuclein Aggregation. Front Cell Neurosci. 2015;9.

99. Jellinger KA. Multiple System Atrophy: An Oligodendroglioneural Synucleinopathy1. J Alzheimers Dis. 62(3):1141–79.

100. Garg N, Smith TW. An update on immunopathogenesis, diagnosis, and treatment of multiple sclerosis. Brain Behav. 2015 Sep;5(9):e00362.

101. Goetz CG, Fahn S, Martinez-Martin P, Poewe W, Sampaio C, Stebbins GT, et al. Movement Disorder Society-sponsored revision of the Unified Parkinson's Disease Rating Scale (MDS-UPDRS): Process, format, and clinimetric testing plan. Mov Disord. 2007;22(1):41–7.

102. Sletten DM, Suarez GA, Low PA, Mandrekar J, Singer W. COMPASS 31: A Refined and Abbreviated Composite Autonomic Symptom Score. Mayo Clin Proc. 2012 Dec;87(12):1196–201.

103. Fujimoto JG, Brezinski ME, Tearney GJ, Boppart SA, Bouma B, Hee MR, et al. Optical biopsy and imaging using optical coherence tomography. Nat Med. 1995 Sep;1(9):970–2.

104. Cifuentes-Canorea P, Ruiz-Medrano J, Gutierrez-Bonet R, peña-garcía P, Sáenz-Francés F, Martínez-de-la-Casa J. Analysis of inner and outer retinal layers using spectral domain optical coherence tomography automated segmentation software in ocular hypertensive and glaucoma patients. PLOS ONE. 2018 Apr 19;13:e0196112.

105. Li S ting, Wang X ning, Du X hua, Wu Q. Comparison of spectral-domain optical coherence tomography for intra-retinal layers thickness measurements between healthy and diabetic eyes among Chinese adults. PLoS ONE. 2017 May 11;12.

106. Tewarie P, Balk L, Costello F, Green A, Martin R, Schippling S, et al. The OSCAR-IB Consensus Criteria for Retinal OCT Quality Assessment. PLoS ONE. 2012 Apr 19;7(4):e34823.

107. Pilotto E, Leonardi F, Stefanon G, Longhin E, Torresin T, Deganello D, et al. Early retinal and choroidal OCT and OCT angiography signs of inflammation after uncomplicated cataract surgery. Br J Ophthalmol. 2019 Jul 1;103(7):1001–7.

108. Cramm M, Schmitz M, Karch A, Mitrova E, Kuhn F, Schroeder B, et al. Stability and Reproducibility Underscore Utility of RT-QuIC for Diagnosis of Creutzfeldt-Jakob Disease. Mol Neurobiol. 2016;53(3):1896–904.

109. Schmitz M, Cramm M, Llorens F, Müller-Cramm D, Collins S, Atarashi R, et al. The real-time quaking-induced conversion assay for detection of human prion disease and study of other protein misfolding diseases. Nat Protoc. 2016 Nov;11(11):2233–42.

110. Kuzkina A, Panzer C, Seger A, Schmitt D, Rößle J, Schreglmann SR, et al. Dermal Real-Time Quaking-Induced Conversion Is a Sensitive Marker to Confirm

Isolated Rapid Eye Movement Sleep Behavior Disorder as an Early α-Synucleinopathy. Mov Disord. 2023 Feb 1;

111. Emmi A, Sandre M, Russo FP, Tombesi G, Garrì F, Campagnolo M, et al. Duodenal alpha-Synuclein Pathology and Enteric Gliosis in Advanced Parkinson's Disease. Mov Disord. n/a(n/a).

112. Cruz-Herranz A, Balk LJ, Oberwahrenbrock T, Saidha S, Martinez-Lapiscina EH, Lagreze WA, et al. The APOSTEL recommendations for reporting quantitative optical coherence tomography studies. Neurology. 2016 Jun 14;86(24):2303–9.

113. Bittersohl D, Stemplewitz B, Keserü M, Buhmann C, Richard G, Hassenstein A. Detection of retinal changes in idiopathic Parkinson's disease using high-resolution optical coherence tomography and heidelberg retina tomography. Acta Ophthalmol (Copenh). 2015;93(7):e578–84.

114. Stemplewitz B, Keserü M, Bittersohl D, Buhmann C, Skevas C, Richard G, et al. Scanning laser polarimetry and spectral domain optical coherence tomography for the detection of retinal changes in Parkinson's disease. Acta Ophthalmol (Copenh). 2015;93(8):e672–7.

115. Mailankody P, Battu R, Khanna A, Lenka A, Yadav R, Pal PK. Optical coherence tomography as a tool to evaluate retinal changes in Parkinson's disease. Parkinsonism Relat Disord. 2015 Oct 1;21(10):1164–9.

116. Albrecht P, Müller AK, Südmeyer M, Ferrea S, Ringelstein M, Cohn E, et al. Optical Coherence Tomography in Parkinsonian Syndromes. PLoS ONE. 2012 Apr 13;7(4):e34891.

117. Fischer MD, Synofzik M, Kernstock C, Dietzsch J, Heidlauf R, Schicks J, et al. Decreased retinal sensitivity and loss of retinal nerve fibers in multiple system atrophy. Graefes Arch Clin Exp Ophthalmol. 2013 Jan 1;251(1):235–41.

118. Schneider M, Müller HP, Lauda F, Tumani H, Ludolph AC, Kassubek J, et al. Retinal single-layer analysis in Parkinsonian syndromes: an optical coherence tomography study. J Neural Transm. 2014 Jan 1;121(1):41–7.

119. Midena E, Bini S, Torresin T, Martini F, Pucci P, Daniele A, et al. Hyperreflective Retinal Spots in Diabetic Eyes with and without Diabetic Macular

Edema: B-Scan and en-face Spectral Domain Optical Coherence Tomography Evaluation. Invest Ophthalmol Vis Sci. 2016 Sep 26;57(12):3252.

120. Choi S, Guo L, Cordeiro MF. Retinal and Brain Microglia in Multiple Sclerosis and Neurodegeneration. Cells. 2021 Jun 15;10(6):1507.

121. Donadio V, Wang Z, Incensi A, Rizzo G, Fileccia E, Vacchiano V, et al. In Vivo Diagnosis of Synucleinopathies. Neurology. 2021 May 18;96(20):e2513–24.

122. Donadio V, Incensi A, El-Agnaf O, Rizzo G, Vaikath N, Del Sorbo F, et al. Skin α-synuclein deposits differ in clinical variants of synucleinopathy: an in vivo study. Sci Rep. 2018 Sep 24;8(1):14246.

123. Donadio V, Incensi A, Piccinini C, Cortelli P, Giannoccaro MP, Baruzzi A, et al. Skin nerve misfolded α-synuclein in pure autonomic failure and Parkinson disease. Ann Neurol. 2016;79(2):306–16.

124. Doppler K, Weis J, Karl K, Ebert S, Ebentheuer J, Trenkwalder C, et al. Distinctive distribution of phospho-alpha-synuclein in dermal nerves in multiple system atrophy. Mov Disord. 2015;30(12):1688–92.

125. Wang N, Gibbons CH, Lafo J, Freeman R. α-Synuclein in cutaneous autonomic nerves. Neurology. 2013 Oct 29;81(18):1604–10.